OPTICAL PATTERN RECOGNITION USING FOURIER OPTICS AND He - Ne LASER SCATTERING TECHNIQUES

BY

MUTHUSAMY N.

LASER TECHNOLOGY PROGRAMME

INDIAN INSTITUTE OF TECHNOLOGY KANPUR

APRIL, 1992

OPTICAL PATTERN RECOGNITION USING FOURIER OPTICS AND He-Ne LASER SCATTERING TECHNIQUES

A THESIS SUBMITTED
IN PARTIAL FULFILMENT OF THE REQUIREMENTS
OF THE DEGREE OF

MASTER OF TECHNOLOGY

BY

M U T H U S A M Y .N

TO THE
LASER TECHNOLOGY PROGRAMME
INDIAN INSTITUTE OF TECHNOLOGY
KANPUR
APRIL, 1992

CERTIFICATE

It is certified that the work contained in the thesis entitl "OPTICAL PATTERN RECOGNITION USING FOURIER OPTICS AND He-Ne LAS SCATTERING TECHNIQUES " by *MUTHUSAMY. N*, has been carried out unde my supervision and that this work has not been submitted elsewhere f a degree.

KK Sharma 30/4/92

(K K SHARMA)

Professor

Laser Technology Programme

Indian Institute of Technology

Kanpur

April, 1992

LTP-1992-M-MUT-OPT

ACKNOWLEDGEMENT

It is a great pleasure to record my sincere thanks to Dr.K.K. SHARMA for his stimulating discussions and suggestions at many stages of my project. To be able to tap his experience on Optics and other fields of interest had been invaluable. He played an integral role in proof reading and styling the English of my entire thesis.

I am grateful to Mr. M. Mani, DEPUTY SECTION HEAD, INSAT, M.C.F. who had been instrumental in getting leave for my studies.

I owe a debt of gratitude to Dr. R. Rangarajan, DIRECTOR, INSAT, M.C.F who had been kind enough to grant and extend leave for my studies.

Special thanks go to Mr. Chakravarthy, PCB lab, Electrical Department for his help in preparing the spatial filters and Photoreduction of my specimen.

Thanks are also due to Librarian and Administrative Officer, FORENSIC SCIENCE DEPARTMENT, Rohini, New Delhi for their hospitality rendered during the period of my Literature Survey.

Om Prakash deserves praise for his painstaking efforts in fabricating all the essential components of my project in no time. I wish to express my sincere thanks to Mr.Sharma and others, CELT workshop.

I express my sincere thanks to Mr. Lal for his voluntary help.

Many thanks to Sharan for his fingerprints and help.

I am grateful to my Friend Sanjeev Dixit for his help, useful discussions and constructive criticisms. His friendship is one of the valuable things I could get here. Thanks also go to my

colleague Arvind who had been patient enough to hear and discuss various points of my project. His association is yet another memorable event in my life.

I thank all my Labmates for their kind cooperation, useful discussion and help.

I also thank Mr. Kuldeep singh and Maharaj Singh for their timely help.

I wish it were possible to thank by name all my colleagues and friends who moved with me during the period of my stay here and made my stay memorable and lively.

Thanks to all my colleagues of INSAT, M. C. F, for their inspiration.

Finally, there are my parents and my brothers, who are the men behind the scenes, made my degree all possible and worthwhile.

MUTHUSAMY. N

TABLE OF CONTENTS

NOMENCLATURE

$\otimes$ = Operation of Correlation

λ = Wavelength

D = Grating Element

E = Electric Field

δ = Path Difference

FDP = Fraunhofer Diffraction Pattern

τ_f = Transmission function

$< >$ = Operation of Averaging in time

FTH = Fourier Transform Hologram

SEM = Scanning Electron Microscope

F, FT = Fourier Transform

Å = 10^{-10} meter

ϕ = Beam Divergence, Phase

I = Energy Density

W = Beam Width

ℓ = Coherence Length

FDPMS = Fraunhofer Diffraction Pattern Modulus Squared

Name : *MUTHUSAMY. N*

Roll No. : 9011606

Degree : M. Tech.

Department : Laser Technology

Thesis Title : Optical Pattern Recognition using Fourier Optics and He-Ne laser scattering Techniques.

Thesis Supervisor : Dr. K. K. Sharma

SYNOPSIS

In recent years a great deal of effort has been devoted to apply Optical Techniques to Pattern Recognition. Optical techniques are very fast and accurate due to the inherent properties of the light beam such as Parallel data flow and Synchronicity. These properties made Parallel processing practicable by the developement of electrical-to-optical interface devices in conjunction with the Computer.

In the present thesis work, effort has been made to identify patterns using Fourier Optics and He-Ne light scattering Techniques. The specimen taken for analysis is fingerprints. These uniquely identify an individual and remain unchanged throughout life unless obliterated by deep-seated injury.

A parallel beam of expanded laser light passing through a fingerprint pattern (object) form its Fourier Transform in the focal plane of the lens, the lens being placed after the object pattern at a distance equal to its focal length. A pinhole camera is placed at the focal (Fourier) plane and the transform of various fingerprint

patterns introduced at the object plane are recorded in a black & white photographic film. The developed film is the negative of the Spatial filter that is desired, so it is contact printed or reversed to obtain positive spatial filter.

In the Spatial Filtering arrangement, the positive spatial filter is introduced in the focal plane of the lens L_1 and the image reconstructed by the Fourier lens L_2, placed at a distance equal to its focal length in the front side of the filter, is observed at the image plane. When the Fourier Transform of the object pattern matches with the transparent portion of the filter, all the spatial frequencies of the object will be transmitted and consequently the image formed will be in exact correspondence with the object. If the filter doesn't match, it blocks some of the (higher) spatial frequencies, thereby introducing distortions in the image. By introducing various filters in the filtering plane, the image formed is photographed. The same process is repeated for different fingerprint patterns. By looking at the image formed for various filters, one can identify the pattern looking for.

In ☺-Fourier method, instead of looking at the image formed by the Fourier Transform lens L_2, a photodetector is kept at the focal plane of the lens L_2 and the detector reading is observed for various filters. Detector output shows maximum only when the F.T of object and the filter introduced matches exactly. Different filters are introduced in the filtering plane and the corresponding detector output is noted. The same process is repeated for various fingerprint patterns introduced at the object plane. From the detector output reading one can identify the pattern looking for.

In the He-Ne light scattering Technique, fingerprints impressed on different metallic surfaces are scanned with the laser beam at an

angle of 30° with respect to the normal. The specimen is kept in a graduated table and is translated at a uniform rate of 5 rpm using a stepper motor. The incident light is reflected from the metallic surface on the other side of the normal and it is focused by a condensing lens on to a photodetector. The variation in the detector output is plotted in a plotter as well as stored in a Boxcar Signal processor. The scanning process is repeated in the same direction, in the identical place but without fingerprint and the detector output is plotted as well as stored. The laser beam scans the same portion of the metallic surface in the beginning as well as in the end of the scanning process and so the shape of the graph should remain identical in those two places of the specimen in both the cases. The graphs obtained in both the cases are matched first and then the second graph is subtracted from the first. The resultant graph gives variation due to fingerprint pattern.

DEDICATED

TO MY

FATHER AND MOTHER

FOR THEIR SACRIFICE

CHAPTER 1

INTRODUCTION

Fingerprint identification is now so widely used and accepted, that without it, the administration of justice and detection of crime would, to say the least, be seriously impeded. This widespread use is a continuing and ever growing tribute to the pioneers in the field. The research work of Sir Francis Galton, Sir William Herschel and Sir Edward Henry in the latter part of the last century laid the foundation upon which the system today is built [1]. Fingerprints are individual and the ridges remain unchanged throughout life unless obliterated by deep-seated injury.

Fingerprints are frequently left behind in burglaries. A recent study [2] revealed that fingerprints are present in almost all the burglary scenes. The latent fingerprints and tool marks are the two most frequently appearing categories of physical evidence at burglary crime scenes. Almost any type of crime can be solved through the recognition of fingerprint and tool marking evidences and subsequent examination and identification in the lab. New scientific procedures for improving the speed, accuracy and reproducibility of fingerprint examinations are desirable. My endeavour in this connection reveals one such method for easy examination.

1.1 FINGERPRINT FUNDAMENTALS AND CLASSIFICATIONS

As is well known, fingerprints uniquely identify an individual. Due to the binary nature of the ridge-pattern images, they constitute a particularly interesting image type. Fig 1.1 shows number of general fingerprint patterns. An initial observation is the fact that the

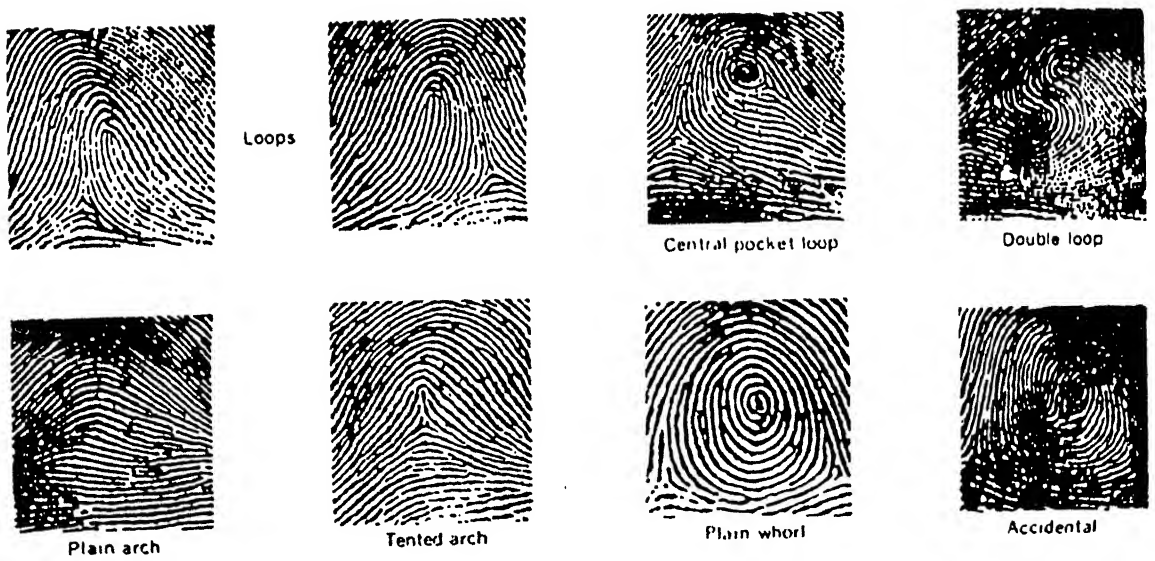

FIG 1.1 GENERAL FINGERPRINT PATTERNS

ridge orientations do change spatially. The individual characteristics that uniquely identify a fingerprint are called minutiae, which are essentially the various types of ridge-pattern deviations as shown below in Fig 1.2.

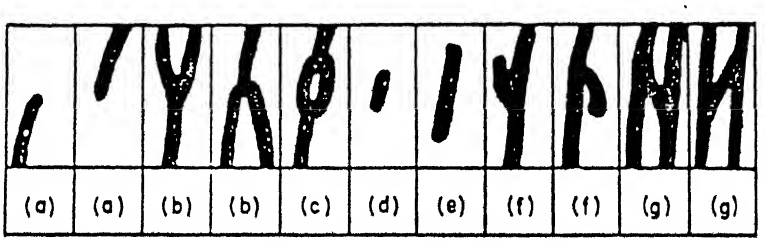

FIG 1.2 SEVEN BASIC TYPES OF FINGERPRINT MINUTIAE

(a) Ridge termination (b) Fork (c) Lake (d) Island
(e) Short independent ridge (f) Hook (g) Cross over

Thus, the basic ridge patterns shown in Fig 1.1 plus the minutiae and their locations on the fingerprint pattern uniquely characterize a fingerprint. As shown in Fig 1.2 three basic types of minutiae are bifurcations,ridge endings and short independent ridges. All ridge

characteristics can be described by combining the basic types. In standard fingerprint patterns there are four main types: Arches, Loops, Whorls and Compounds (see Fig 1.3). There are, of course, variations of these, but a finger impression can be allocated under one of these four types.

As majority of us have eight fingers and two thumbs, the possible combinations of patterns on the ten digits is well over a million, and of course, this number of primary groups was too unwieldy for easy working. Sir Edward Henry however, took into account the incidence of patterns, for he found that Arches comprise approximately 5% of all

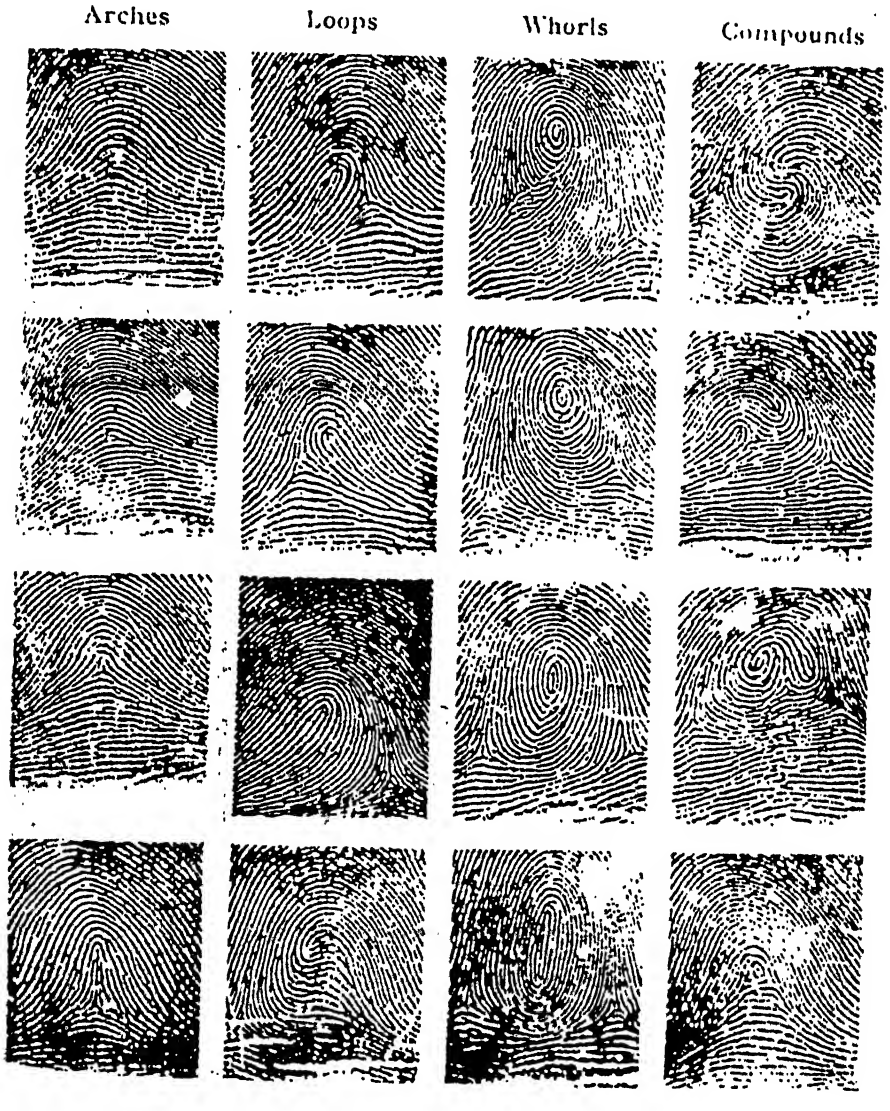

FIG 1.3 STANDARD TYPES OF FINGERPRINT PATTERNS

finger impressions. Loops 60% and Whorls and Compounds 35% and for the purpose of the first split, he grouped Arches and Loops together denoting them with letter "L" and Whorls and Compounds together using "W". The alternate pattern for an individual digit will now be "L" or "W" and the possible combinations on the ten digits is therefore 1,024. He further found that by making the digits in pairs, the right thumb and right forefinger as the first pair and so on down to the left ring and left little finger as the fifth pair, that a cabinet containing 32 sets of 32 pigeon holes arranged horizontally would provide a pigeon hole for each combination of "L" and "W" patterns and he provided this key idea and the chart is illustrated in Fig 1.4. This gives us basic idea of classifying different fingerprints based on its shape.

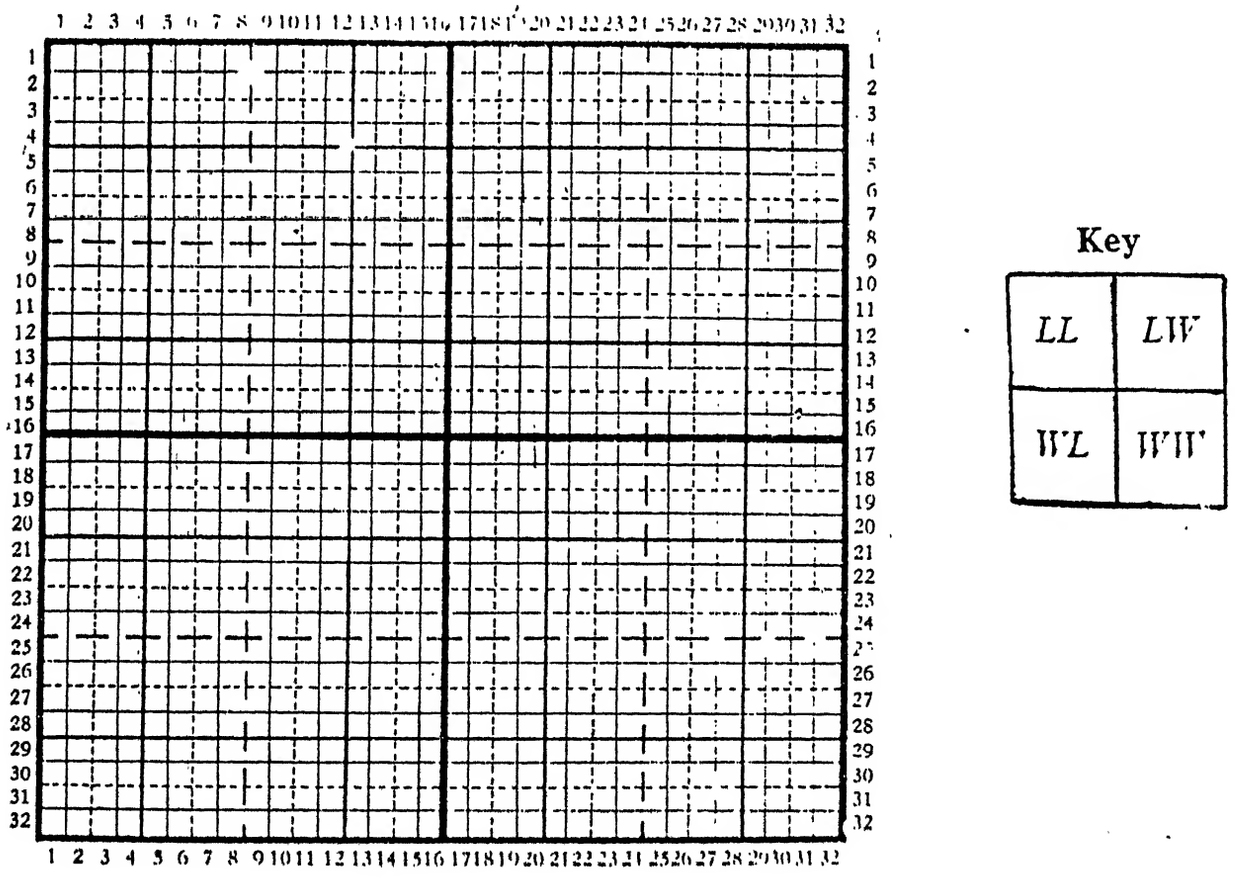

FIG 1.4 CHART FOR FINGERPRINT CLASSIFICATION

The impressions of the ten digits are taken in pairs in the following order: (1) Right Thumb and Right Index ; (2) Right middle and Right Ring (3) Right little and left Thumb (4) Left Index and Left Middle (5) Left Ring and Left Little. All impressions are held to be divisible into 2 types, Loops (which include Arches) and Whorls. Given ten impressions in the above order, they can be expressed by some such formula as the following: LW-WL-LL-WW-LW where L=Loop; W=whorl. The key indicates that one-pigeon hole out of 1024 of the Bureau where a card with the above formula will be found. Referring to the key, LW is in top right hand square, therefore we proceed to square defined by the broad continuous lines and by the horizontal numbers 17 to 32 and vertical 1 to 16. Taking the next pair WL we see from the key that is in bottom left square of $\frac{17\text{-}32}{1\text{-}16}$ .i.e.,in the square defined by continuous and broken lines and by horizontal figures 17-24 and vertical 9-16. The next pair LL is in left top corner of this $\frac{17\text{-}24}{9\text{-}16}$ square, i.e., in sqaure defined by one broad continuous, one broad broken, and two meidum continuous lines, and by horizontal figures 17-20 and vertical 9-12. The next pair WW is in right hand bottom corner of this $\frac{17\text{-}20}{9\text{-}12}$ square, i.e., in square marked by two broken and two continuous lines and by horizontal figures 19-20 and vertical 11-12. Finally, the last pair LW is in top right hand corner of this $\frac{19\text{-}20}{11\text{-}12}$ square, i.e., is in pigeon hole $\frac{20}{11}$. Any other combination of impression can be similarly located.

1.2 LITERATURE SURVEY

Fingerprints have been studied more closely over the years and they have been well classified according to their ridge patterns. But unfortunately no method can exactly identify a particular fingerprint. There are various techniques for the identification of fingerprints which can be broadly classified into four groups.

1.2.1 MICROSCOPIC STUDY

The standard procedure employed by fingerprint examiners in comparing crime scene marking with those from the suspected ones has not changed significantly for several decades. The primary examination technique involves the simultaneous examination of the evidence print and the test print under a comparison microscope. The examiner applies lighting at various intensities and angles to bringout the desired contour variations. Different areas of both fingerprint patterns are compared and adjusted until one continuous line network is formed. There will rarely be a case where all the striae of the two samples will match exactly. The examiner must therefore judge judiciously how many matching striations or the ratio of the matching striae to the total striae are sufficient to constitute an identity. The visual microscopic matching process is influenced by skill and persistence of the examiner in adjusting the fingerprints and his source of illumination.

1.2.2 SCANNING ELECTRON MICROSCOPE (SEM)

The SEM uses a narrow 20-100 Å diameter focussed beam of electrons accelarated from 1,000 to 50,000 volts which is scanned over a sample surface in a square pattern similar to the picture pattern generated in a television tube. When this beam impacts the sample surface several things occur which can yield information about the surface. Electons from the structure of the sample (i.e., secondary electrons) can be collected at each point of the scanned pattern and the intensity of the secondary electrons at each point can be amplified by a photomultiplier tube and subsequently displayed on a cathode-ray tube whose phosphor surface is scanned in synchrony with the beam scanning the sample surface. The result is a topographical picture of the sample area being scanned. The high energy electrons

from the primary beam which are reflected from the sample surface can be collected and are of particular value to fingerprint work because electrons are less susceptible to charging artefacts that occur on non-conductive or poorly conducting surfaces where prints are often found.

Fingerprints consisting of mostly body oil are deposited on glass which are then cemented to SEM stubs with silver conducting cement. They are examined in the SEM before and after ageing, weathering and heating, with and without gold coating. Under certain condtions fingerprints can be successfully recorded using the SEM where extreme difficulties are encountered in traditional methods. The photographs show that SEM works well on conductive and non-conductive surfaces but when the surface containing fingerprints are exposed to sun light and rain, a coat of material is deposited on the print which becomes opaque to electron penetration. The size of the object is also limited to 4 inches in any dimension.

1.2.3 DIGITAL IMAGE PROCESSING TECHNIQUE

Modern Communications require the transmission, storage and display of information in pictorial form, both for data as well as for information in actual "image" form. Digital implementations are likely to be the most practical in general cases, where certain current limitations are surmounted.

The essential components of an image processing system are illustrated in Fig 1.5. Examples of typical input, output storage and transmission systems are listed in Table 1. The most interesting component, however, is probably the processor itself.

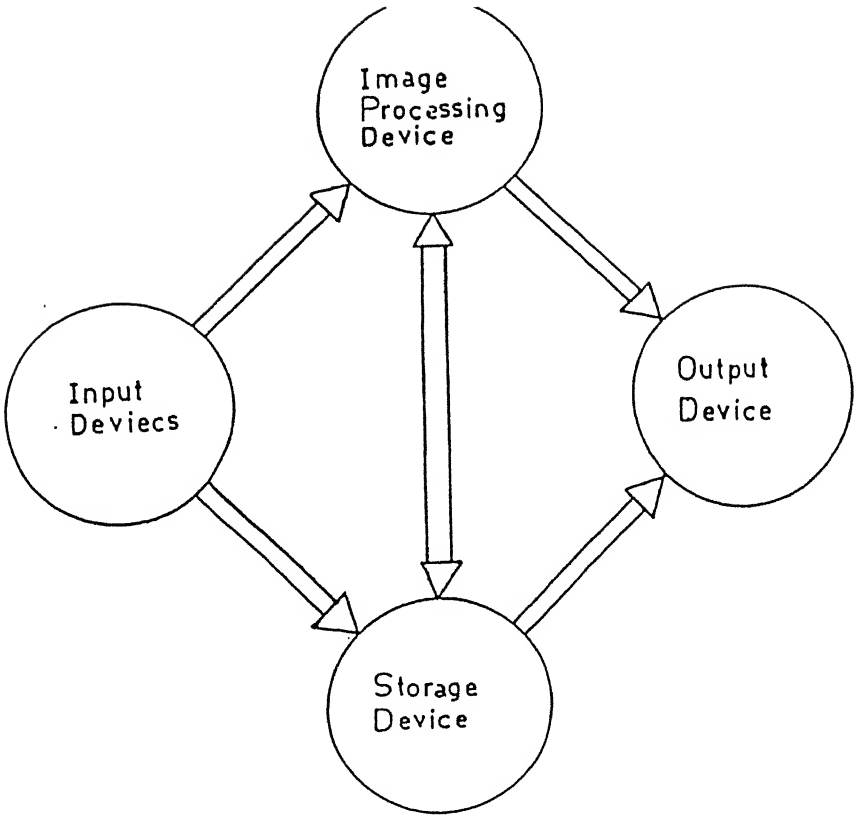

FIG 1.5 IMAGE PROCESSING SYSTEM CONFIGURATION

TABLE 1

INPUT DEVICES	OUTPUT DEVICES
TV Camera	TV display
Solid state array	Line printer
Radiation detector	Graphics display
Radar scanner	Plasma display
	Matrix printer

STORAGE DEVICES	TRANSMISSION CHANNELS
Magnetic tape	Laser beam
Magnetic disc	TV Channel
Holographic memory	Data link
Video disc and tape	Voice telephone
	Teletype

Digital processing calls for the use of scanning of the photographic images. Images inherently consists of two-dimensional analog signals concerned with position, brightnesss and colour. The image is normally formed as a large square array of picture element (pixels) usually 256 x 256 or 512 x 512, although even larger arrays are increasingly available. Each pixel has a particular brightness or grey level, value assigned to it. Usually one of the 256 possible levels for a typical 8-bit display device. The image is digitized and the pixel value along with their associated positions are entered as numbers into a computer. To analyse the content of the image lengthy computations are performed. The data obtained from a computer are sequential digital values, so they are transduced to two-dimensional analog signals that is continuous-tone pictures. Cathode Ray Tube is used to display two-dimensional pattern of the picture.

ADVANTAGES

This processing is flexibile and has high degree of precision. Digital computers, however, are capable of applying a wide range of complicated algorithms, some of which would be difficult to implement optically. Other advantages include high precision, repetability and transferability of software.

DISADVANTAGES

Unlike optical image processing, for example, which is readily implemented with only three basic components (laser, lenses and photographic film), it is evident that digital image processing requires the use of much larger number of basic components and therefore the solutions of many more and different problems. High speed, parallel processing and large storage capability of optical

systems makes it hard for Digital computers to compete in the implementation of processes involving Fourier transformation such as image deblurring. Much can be learned, in fact, from optics which should be of fundamental interest for the digital implementations.

1.2.4 OPTICAL IMAGE PROCESSING TECHNIQUE

The Optical processing technique using coherent light illumination comes under Fourier optics. When the input plane is illuminated by a plane wave, the Fourier transform of the input transmittance is generated automatically in the rear focal plane of the positive lens. In addition the transform of a product of two pattern transforms is equivalent to the cross-correlation (mentioned below) of the two patterns. Since the Fourier transform is the basis of the correlation and convolution theorems of communication theory dealing with signal detection, the ability of a coherent system to perform this transform lends it naturally to optical processing tasks of pattern recognition and image analysis. There has been an apparently erroneous impression that optical processing deals only with actual optical images as such. In fact, optical computing is used to synthesize and process images and signals acquired with radiations which range from X-rays and electron beams to Radio and Radar waves (As in synthetic aperture coherent radar) and indeed signals and images acquired with ultrasonic radiations as well [3].

ADVANTAGES

The optical processing is attractive and very fast because it has the advantage of 2-dimensional display and parallel processing. Parallel data flow and synchronicity are natural properties of an expanded light beam. The elements of a pattern encoded on a beam all arrive at the same time at several planes of the optical system through which the beam passes. The two dimensional data flow is made

possible and practicable by the development of electrical-to-optical interface devices in conjunction with the computer.

In the area of optical pattern recognition there are two major methods (Fig 1.6) which are of vital interest. They are:

1. Template matching
2. Feature extraction

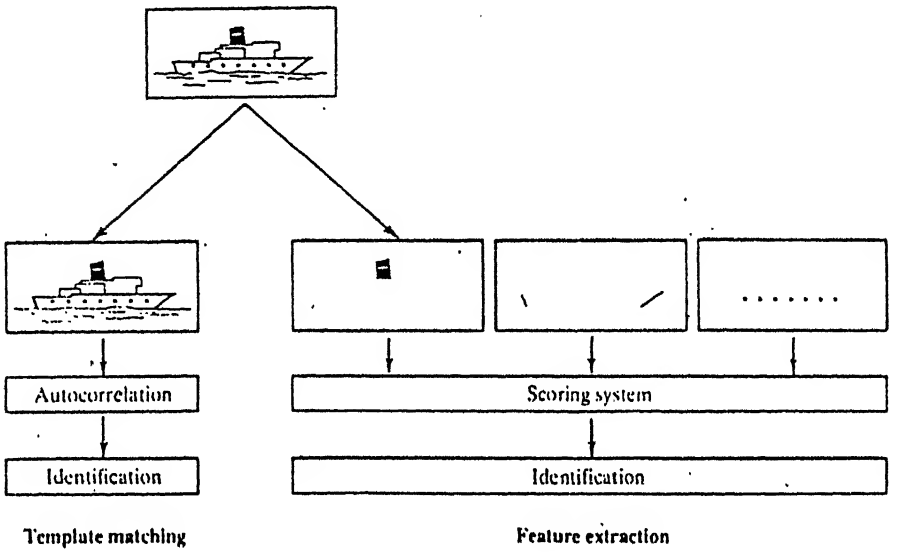

FIG 1.6 PATTERN-RECOGNITION TECHNIQUES

1.2.4.1 TEMPLATE MATCHING

Template matching refers to the comparison of the test pattern with a number of stored patterns until an exact match is found. It is a top-down process in the sense that the trial procedure does not depend on the test pattern in any way. In the Fig 1.5 comparison of a ship sailing in a sea is done with the test pattern . The output of the autocorrelator indicates maximum when proper match between those two patterns is found and this leads to identification of the pattern. Template matching is both computationally and memory intensive, but computation can be performed very quickly using optical technique and auto-correlation (mentioned below) can take care of sensitiveness of the exact location of the object. The optical technique has an

advantage of simultaneous pattern registration and recognition.

CORRELATION

Correlation is one of the most ubiquitous of all signal and data treatment tools in use today. It is essentially a method for assessing and specifying mutual relationships where these take the form of similarities or coincidences.

Correlation describes the degree to which two functions "match-up" as they are shifted relative to each other.

AUTOCORRELATION

The autocorrelation function of the function $g(\xi,\eta)$ is defined by the expression

$$\int_{-\infty}^{+\infty}\int_{-\infty}^{+\infty} g(\xi',\eta')\, g^{*}(\xi'-x,\eta'-y)\, d\xi'\, d\eta' \quad \ldots\ldots\ldots\ldots\ldots\ldots(1)$$

where ξ,η being variables of integration

This above equation is symbolically written as

$$g(\xi,\eta) \otimes g^{*}(-x,-y) \quad \ldots\ldots\ldots\ldots\ldots\ldots\ldots\ldots(2)$$

The autocorrelation will always be largest at x=0. This represents the condition where the function is not shifted with respect to itself. Here the product in the integrand is as large as it can be for all values of the range of integration. As the relative shift increases, the autocorrelation will drop off according to the extent and shape of the original function.

EXAMPLE

Consider the example of a slit function (Fig 1.7) whose Fourier

transform is represented in Fig 1.7 (a). The autocorrelation function is determined by calculating the variations of the shaded area in Fig 1.8 as a function of ξ. We have here designated the width of the slit as ξ_0' in order not to cause any confusion with the variable of integration ξ'. Fig 1.9 represents the autocorrelation function of $F(\xi)$

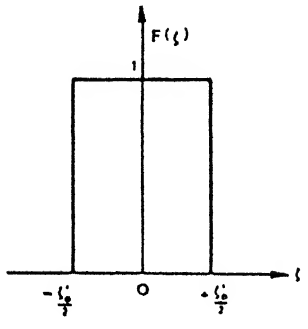

FIG 1.7

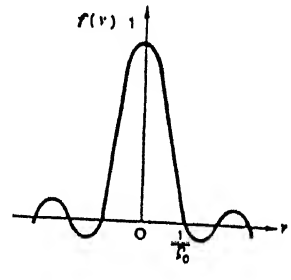

FIG 1.7 (a)

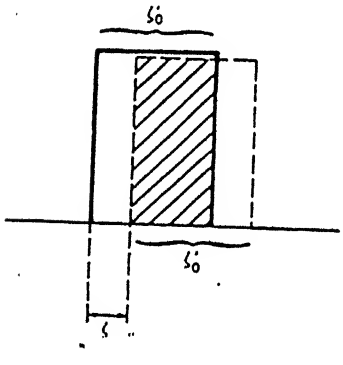

FIG 1.8

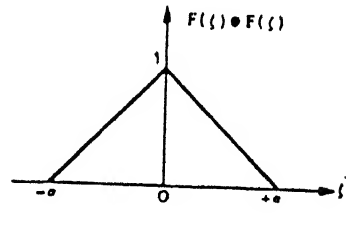

FIG 1.9

CROSS-CORRELATION

To compare two different functions cross-correlation is used. Cross-correlation of two functions $f_1(x,y)$ and $f_2(x,y)$ in two dimensions takes the form

$$f_1 \otimes f_2 = \int_{-\infty}^{+\infty} \int_{-\infty}^{+\infty} f_1(x',y')\, f_2^*(x'-x,\, y'-y)\, dx'\, dy' \quad \ldots\ldots\ldots\ldots (3)$$

ADVANTAGES

The advantages of the cross-correlation technique for template matching are

1. The matching is independent of the test pattern location
2. The signal-to-noise ratio is optimum for detection in white noise situation [4].

1.2.4.2 FEATURE EXTRACTION

Feature extraction starts from the test pattern and measures a limited number of features that are known, in advance, to be a good descriptor for the pattern. In the Fig 1.6 top figure (ship sailing on the sea) is the test pattern. It is compared with some of the features which are known already. The unknown features can be extracted from the comparison process and the identification of the actual picture can be done. This is a data driven process but bottom-up. In this process the memory requirements are less severe than template matching and hence a microcomputer can be used for low-level vision tasks. For high level tasks artificial intelligence techniques are used. The basic problem with this feature extraction technique is that important information may be lost in the extensive data reduction at the pre-processing stage.

1.2.5 COHERENT LIGHT SCATTERING TECHNIQUE

When a collimated beam of coherent light falls on a metal surface it gets scattered and diffracted. Here in the course of discussion we avoid the effect of diffraction since it does not produce any appreciable change in the output of the photodetector when it is focussed by a condensing lens.

The direction of scattering of the collimated light is dictated

by the nature of surface. If the surface is smooth then all rays of a parallel beam of incident light obey laws of reflection and therefore reflects as a parallel beam. In the case of granular or rough surface the laws of reflection is obeyed locally and the microscopic granular surface will reflect rays in various directions and thus diffuse scattering of the originally parallel rays of light. Every plane surface will produce some such scattering since a perfectly smooth surface is unattainable in practice.

The intensity of scattered light depends upon the roughness height,spatial wavelength of roughness, wavelength of incident light and angle of incidence of the light beam. Since lasers are highly directional, intense and monochromatic, scattering of light by the surface gives us information about the nature of surface and the pattern present on it.

1.3 POTENTIAL APPLICATIONS OF OPTICAL PATTERN RECOGNITION

Optical pattern recognition technique has reached a degree of practical perfection in real-world cases it finds applications in all frontiers of science and engineering. Some of them are cited below with examples.

1.3.1 COHERENT OPTICAL PROCESSING

(A) Character Recognition:

A particular application of optical processing that has been of interest for many years is Character recognition [5]. Fig 1.10 shows a typical optical system used for this.

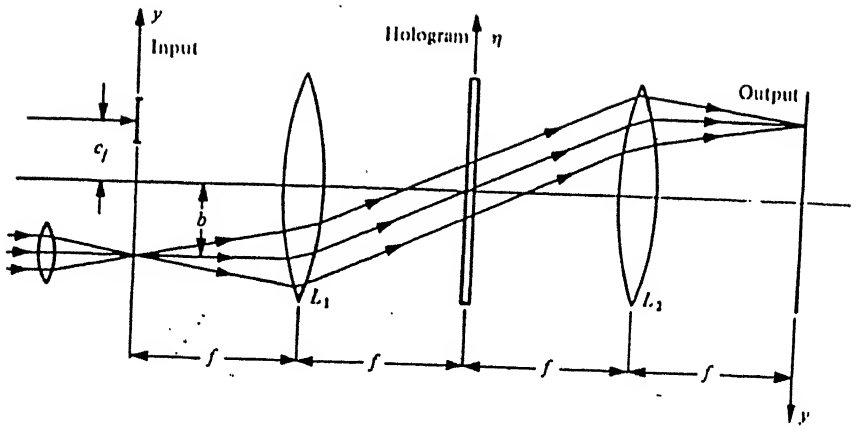

FIG 1.10 OPTICAL SYSTEM USED FOR CHARACTER RECOGNITION

To produce a matched filter, a transparency of the set of characters to be identified is placed in the input plane and a hologram of this transparency is recorded in the Fourier transform plane using a point reference source. The hologram is replaced, after processing, in exactly the same position in which it was recorded and illuminated by a single character of the set centered on the axis. If the autocorrelation function of the character presented is sharply peaked, the image plane will have a bright spot of light. All other patterns which do not match will give "parasitic response" in the image plane.

(B) Biological studies:

A valuable application of Coherent Optical Processing is the analysis of electron micrographs of large biological molecules by optical diffraction, using the electron micrograph as a diffraction mask [6].

An electron micrograph of a tubular structure found in a form of bacteriophage. The outer coating of the tube is composed of protein molecules of molecular weight 50,000 and arranged in a helix like a coil spring. To obtain this picture the specimen had first been

embedded in an electron-dense medium. The medium scatters electrons more efficiently than the protein, and by occupying the holes and crevices in the surface it throws the surface structure into relief. However, tubular specimens like this become flattened when prepared for electron microscopy, and the details of the front and back tube become superimposed. In Fig (b) and (c) we can see how images can be separated. The optical diffraction pattern of (a) is shown in (b). Circles have been drawn round the diffraction spots that could be identified as corresponding to the structure of one layer of the tube. With a mask that allowed only these to proceed to the image plane the picture shown in (c) was obtained. The arrangement of individual molecules can now be seen clearly.

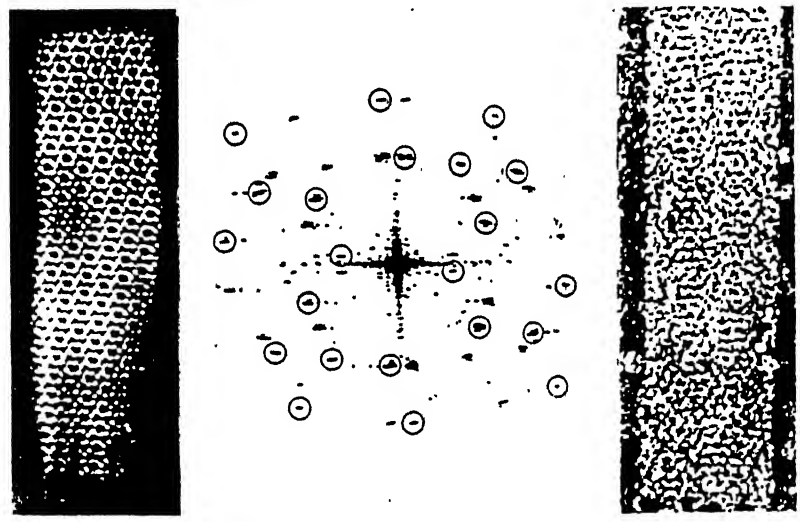

FIG 1.11 OPTICAL FILTERING IN ELECTRON MICROSCOPY

(C) SATELLITE IMAGERY

(1) Object motion analysis:

The specific application considered using optical correlation application is cloud motion analysis [7]. A scanned photograph from the ATS III weather satellite of the cloud pattern over California and part of central Mexico is shown below in Fig 1.12 (a). If the Fourier

Transform Hologram (FTH) of the first frame [Fig 1.12 (b)] in a sequence of these photographs is formed and correlated with the second frame of data [Fig 1.12 (c)], a strong correlation peak is expected [Fig 1.12 (e)], if there is no motion of the cloud patterns between frames. If all of the cloud patterns moved with an equal velocity between frames, the location of the correlation peak would shift accordingly as shown in Fig 1.12 (f). In practice, cloud patterns move in different directions with different velocities. To analyse this motion, various cloud pattern regions were sequentially isolated as shown encircled and numbered in Fig 1.12 (a). The location of their peaks were then measured and converted to velocity vectors. The resultant plot of the velocity vectors or displacements of the indicated regions in the image are shown in Fig 1.12 (g) at half hour and full hour intervals.

FIG 1.12 (a) ATS III WEATHER SATELLITE IMAGE WITH OVERLAY OF VARIOUS SECTIONS

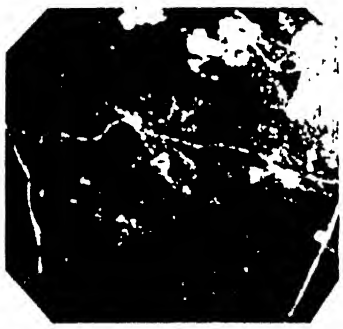

FIG 1.12 (b)
ORIGINAL PICTURE OF
THE CLOUD

FIG 1.12 (c) ANOTHER CLOUD
PICTURE TAKEN AFTER A SHORT
TIME (b) WAS TAKEN

FIG 1.12 (d)
A SMALL SECTION
OF THE CLOUD PICTURE

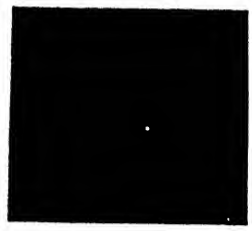

FIG 1.12 (e)
CORRELATION BETWEEN
(a) AND (c)

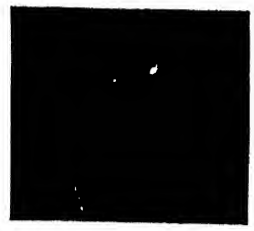

FIG 1.12 (f)
CORRELATION BETWEEN
(b) AND (c)

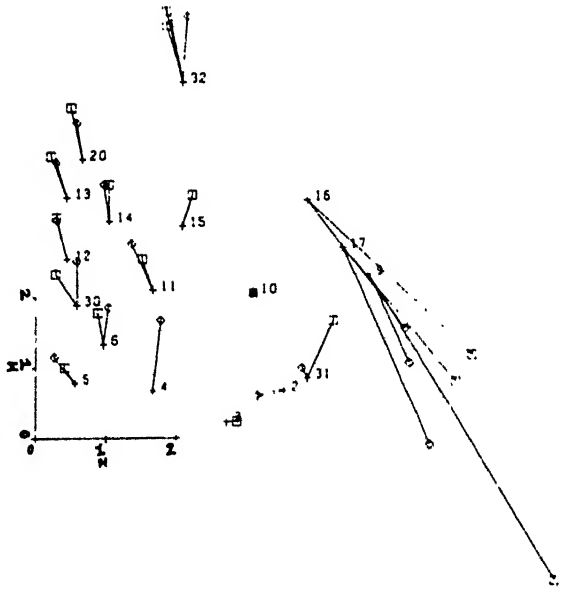

FIG 1.12 (g) WIND VECTOR DIAGRAM OBTAINED FROM THE MOVEMENT OF CORRELATION PEAKS

(2) DECODING BY FOURIER TRANSFORM:

If a meterologist wishes to find out oceanic wind conditions, the direction and magnitude of the wind on the surface of the ocean can be determined from the shape of the ocean waves. The period and the direction of the waves are decoded from the aerial picture as follows. The Fourier transform of a portion of an aerial photograph is made, as shown in Fig 1.13 (a). The transform pattern has a spread in a direction perpendicular to the ocean wave pattern and the amount of spread is used to determine the spatial frequency distribution of the ocean wave. Fig 1.13 (b) shows the aerial picture amalgamated with the Fourier transform of its local regions obtained in the manner described above. From the figure, the direction of the surface wind and period of the ocean waves may be interpreted.

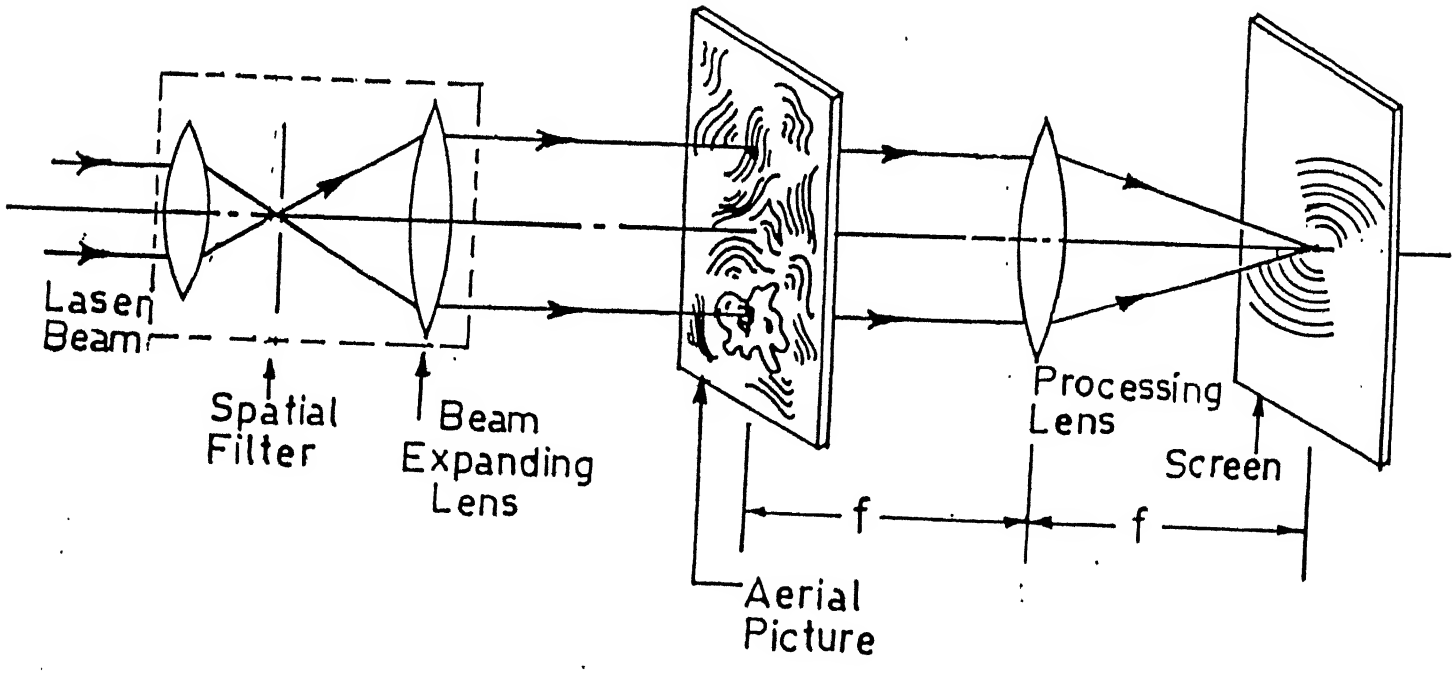

FIG 1.13 (a) A METHOD TO OBTAIN FOURIER TRANSFORM OF OCEAN WAVE PATTERN

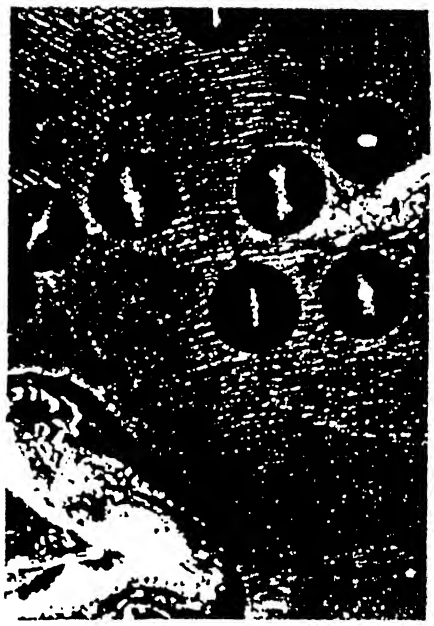

FIG 1.13 (b) AERIAL PICTURE AMALGAMATED WITH THE FOURIER TRANSFORM OF LOCAL REGION OF THE AERIAL PICTURE

1.3.2 INCOHERENT OPTICAL PROCESSING

(A) PCB Inspection:

(B) Character Recognition:

1.4 ORGANISATION OF MY THESIS

According to our survey no worthwhile effort has been made to identify fingerprints using Optical Correlation Technique (OCT). However using Fourier transform Holographic method fingerprint detection is carried out and satisfactory results have been obtained.

In my thesis work however, effort is channelised to identify different fingerprints using coherent optical processing and spatial filtering and He-Ne light scattering techniques. My thesis is organised as follows.

Chapter 2 gives Theoretical background of Fraunhofer diffraction and spatial filtering technique. The experimental details, procedure adopted are discussed in chapter 3 while results and discussions are the subject of chapter 4.

Chapter 5 presents conclusions and further suggestions.

In chapter 6 we explain the experimental setup adopted to carry out the investigation of coherent light scattering using a He-Ne laser .

Chapter 7 discusses the results obtained and its origin, while conclusions drawn and suggestions for further improvements are the subject of Chapter 8.

CHAPTER 2

THEORETICAL BACKGROUND

INTRODUCTION

This chapter aims to cite Fraunhofer diffraction pattern of some simple and multiple shapes and present Fourier transformation by Fraunhofer diffraction. Also covered in this chapter are the need for coherent system and inherent property of Fourier transformation of the lens. Some of the unique characteristics of Fraunhofer diffraction pattern are covered in section 2.6. Finally Image formation and spatial filtering techniques are discussed in detail in the subsequent sections.

2.1 PATTERN RECOGNITION SYSTEM

The diffraction pattern sampling for classifying pattern in photographic transparencies is an important milestone in the area of pattern recognition.

The features of the diffraction pattern correspond to the features of the original photographic images which leads to recognition of the pattern. On the basis of this one can design a sampling system which will preserve this information. The study of the resulting sampled information gives us how they relate to the diffraction pattern. The basic pattern recognition system configuration is shown in Fig 2.1.

The processor processes the photographic input, extracts what information it can and passes this on to the decision processor which could be a computer. The output of this decision processor is the

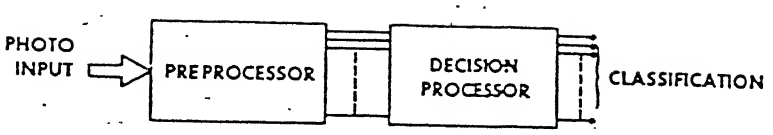

FIG 2.1 PATTERN-RECOGNITION SYSTEM CONFIGURATION

desired classification. Diffraction pattern sampling is intended to serve as a preprocessor for such a system. The decision processor must then use this sampled information to arrive at the desired classification.

2.2 FRAUNHOFER DIFFRACTION PATTERN

All patterns existing in nature can be thought of as a combination of straight and curved diffraction gratings. Similarly, a fingerprint can be fancied as a series of circular and rectangular gratings (see fig 2.2 (a) & (b)). Before considering the diffraction pattern of fingerprints it is worthwhile to consider diffraction pattern of some simple shapes such as circular and rectangular apertures which form the building block of the fingerprint. Subsequently diffraction pattern of some complex shapes are also considered. The kind of diffraction which satisfies our requirement is of Fraunhofer type and hence future discussions on diffraction will be based on Fraunhofer diffraction.

Fig 2.2 (a)

Fig 2.2 (b)

FIG 2.2 FINGERPRINT PATTERN

2.2.1 SOME SIMPLE SHAPES:

Fig 2.3 shows a simple rectangular aperture with dimensio "a","d" and its Fraunhofer diffraction pattern modulus square (FDPMS). Since physical sensors such as eye, film, photoelectric cell etc., senses only intensity, power spectrum of the scan area's transmission function is taken. That is denoted as FDPMS. Th intensity of the FDP along the direction corresponding to the width o the rectangle has the form $\left(\frac{\text{Sin } x}{x} \right)^2$ where x is given by

$$x = \left(\frac{\pi d}{\lambda} \text{ Sin } \alpha \right)$$

d = Width of the slit

λ = Wavelength of the monochromatic light used

α = Angle between optical axis and line drawn from the lens center to the point x in the focal plane of the lens

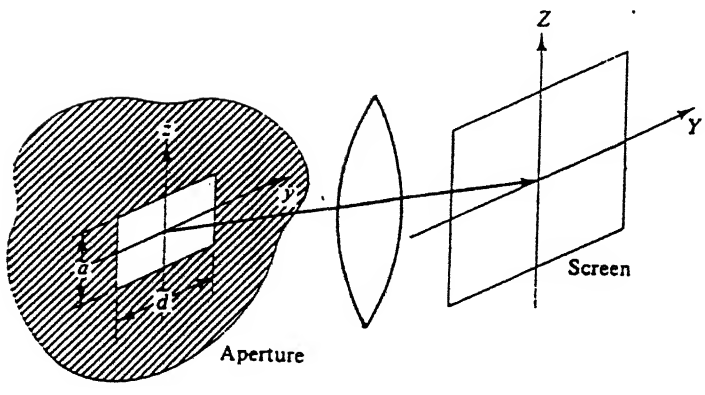

FIG 2.3 (a)

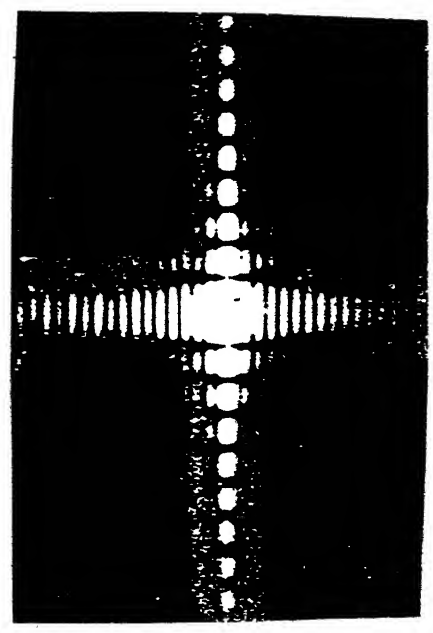

FIG 2.4 (b)

FIG 2.3 (a) GEOMETRY OF A RECTANGULAR APERTURE

FIG 2.3 (b) ITS FRAUNHOFER DIFFRACTION PATTERN

Next look at the circular aperture [Fig 2.4 (a)]. The diffraction pattern is shown in Fig 2.4 (b). This contains a central peak known as Airy disc surrounded by successively weaker symmetric rings.

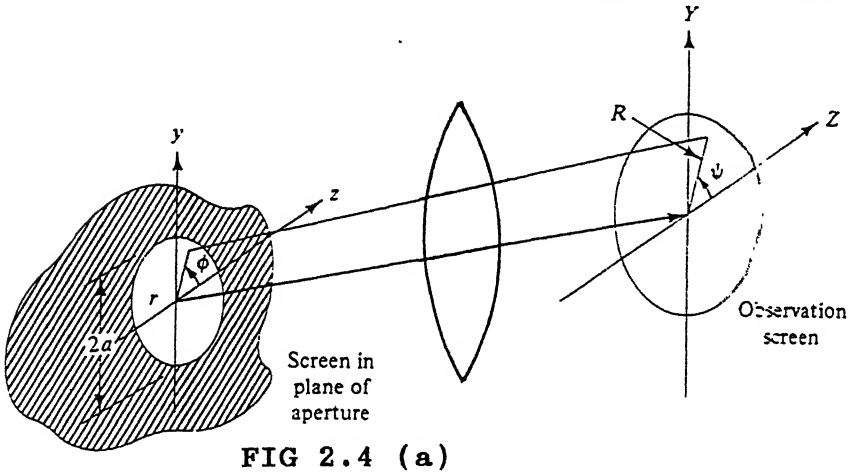

FIG 2.4 (a)

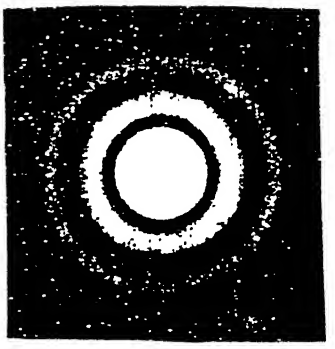

FIG 2.4 (b)

FIGURE 2.4 (a) GEOMETRY OF A CIRCULAR APERTURE

FIGURE 2.4 (b) ITS DIFFRACTION PATTERN

2.2.2 COMPLEX SHAPES

Scan Area From Satellite Photographs:

Fig 2.5 through 2.10 are the scan-areas of the natural terrain photographed from a satellite camera.

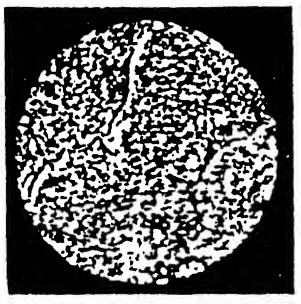

FIG 2.5 (a) NATURAL TERRAIN

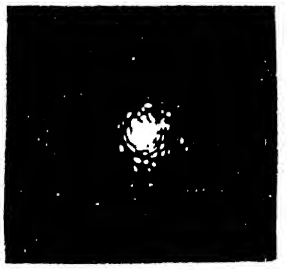

FIG 2.5 (b) ITS FDPMS

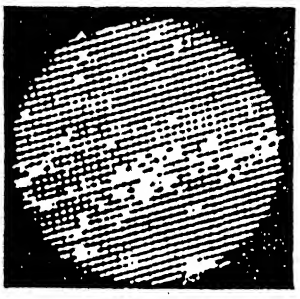

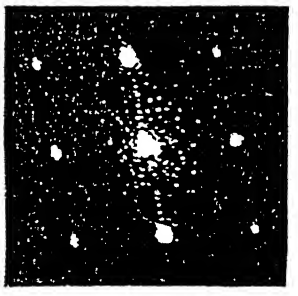

FIG 2.6 (b) ITS FDPMS

FIG 2.7 (a) ROADWAY WITH TERRAIN BACKGROUND

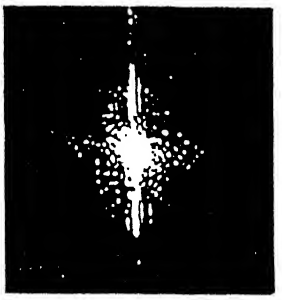

FIG 2.7 (b) ITS FDPMS

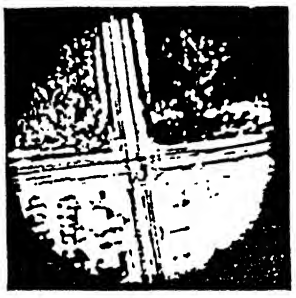

FIG 2.8 (a) ROAD INTERSECTION

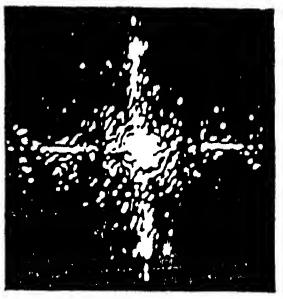

FIG 2.8 (b) ITS FDPMS

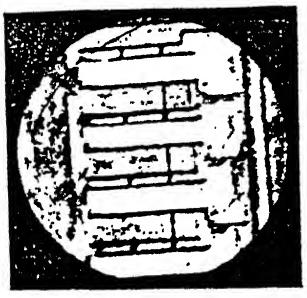

FIG 2.9 (a) COMPLEX LARGE BUILDINGS

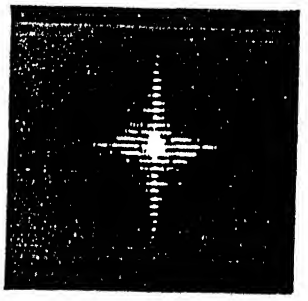

FIG 2.9 (b) ITS FDPMS

An important fact to extract from the above cited figures is that every pattern in the scan area will have its own diffraction pattern and each of these will be superimposed, centered on the optical axis. The FDP is very vital since the scan area is decomposed into its basic building-block patterns and the contribution of each of these to

the FDP is centered on the optical axis of the system no matter where the pattern is located within the scan area.

2.3 FOURIER TRANSFORMATION BY FRAUNHOFER DIFFRACTION

Fourier transformation by Fraunhofer diffraction is the starting point to Fourier optics in Pattern recognition. In the Fig 2.10, line labelled X represents side view of a plane in which x is parallel to X and y is normal to the paper. Suppose this plane is illuminated with parallel coherent monochromatic light at an angle θ . Consider a ray incident on this plane at x=0. At a distance δ backwards along this ray, the phase differs by $\frac{2\pi\delta}{\lambda}$ from the phase at x=0, where λ is the wavelength of light. Since the wavefront is plane, the phase at Q is the same as the phase at P and let x be the distance of Q from

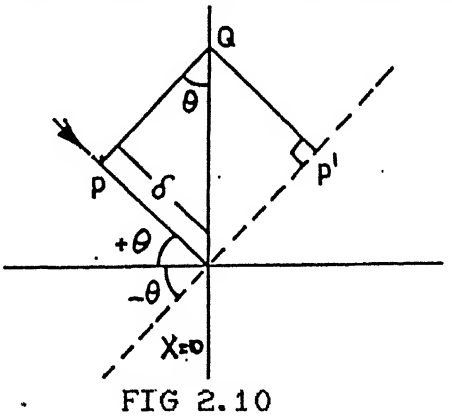

FIG 2.10

x=0. Now δ = x Sinθ and it is convenient to define $\alpha = \left(\frac{2\pi x \sin\theta}{\lambda}\right)$ Thus if the Electric field at x=0 is $ae^{i\omega t}$, then field at P and Q is $e^{i(\omega t-\alpha x)}$. Suppose the plane is also illuminated with parallel coherent monochromatic light with the same wavelength as before, but at an angle $-\theta$, as indicated by the dotted line in the Fig 2.10 such that the phase of the $+\theta$ and $-\theta$ beams of light is the same at x=0. At the point Q the phase of the light from $-\theta$ beam is the same as the phase at P ', which is $\left\{\frac{2\pi\delta}{\lambda} = \alpha x\right\}$ ahead of the phase at x=0. The total complex field at Q due to both beams is

$$a\,e^{i(\omega t - \beta x)} + a\,e^{i(\omega t + \beta x)} = a\,e^{i\omega t}\,(\,e^{i\beta x} + e^{-i\beta x}\,)$$

$$= 2a\,e^{i\omega t}\,\mathrm{Cos}\beta x \quad \ldots\ldots\ldots\ldots\ldots(4)$$

This is the complex field distribution at any point (x,y). Suppose now that the x,y plane contains a photographic transparency or mask whose transmission coefficient is 2 Cosβx. If the x,y plane is illuminated with parallel monochromatic coherent light, of field a $e^{i\omega t}$, in a direction perpendicular to the x,y plane, the light emerging from the mask has field distribution $2ae^{i\omega t}$Cosβx. But this is precisely what would happen if two waves were travelling at $\pm\theta$. From the equation (4) we see that the angle θ depends not only on the wavelength of light but also on the wavelength of the transmission coefficient of the transparency.

If the x,y plane contains a mask which has a periodic transmission coefficient, for instance if the mask is a transparency of fingerprint then the mask can be regarded as the sum of an infinite number of sinusoidal masks, there being one sinusoidal mask per fourier component of the periodic mask. Thus for each Fourier component we get two plane waves in the direction $\pm\,\theta$, where θ depends on the wavelength of the Fourier component in accordance with equation (4). The complex amplitude of these $\pm\theta$ waves depends on the complex amplitude of the corresponding Fourier component.

If we focus these waves by means of a perfect lens, the amplitude at a given point in the focal plane depends on the amplitude of the wave emanating in that particular directiom from the mask. Thus the complex amplitude at a given point in the focal plane of the lens depends on the complex amplitude of a single fourier component of the mask. If, in Fig 2.10 the focal length of the lens L_2 is f_1 then the complex amplitude at a point R in the focal plane which is at a

distance u = f Tan θ from the optic axis depends on the complex amplitude of the Fourier component which is associated with the angle θ. The spatial distribution i.e., the pattern of complex amplitude in the focal plane is the Fourier transform of the pattern which is embodied in the mask. The pattern in the focal plane is the Fraunhofer

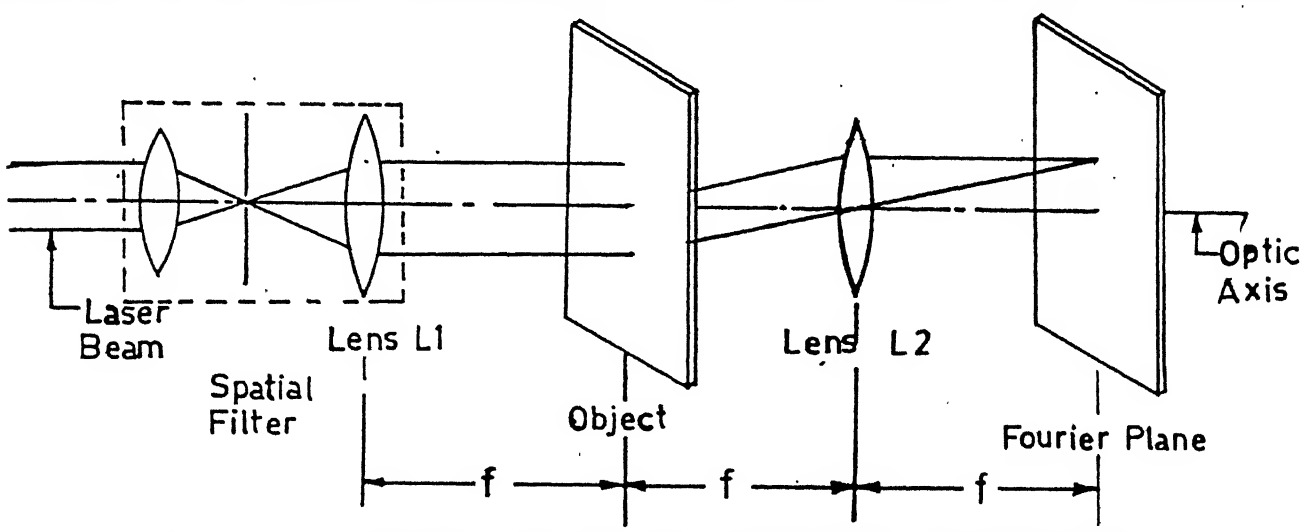

FIG 2.11 A SIMPLE SET-UP FOR FRAUNHOFER DIFFRACTION

diffraction pattern of the mask. The focal plane of the lens L_2 is known as the Fourier plane or Fraunhofer plane of L_2 alternatively.

Again back to Fig 2.10 ,when x,y plane is illuminated from $+\theta$ and $-\theta$ if we retard the phase of the light in the $+\theta$ beam by ϕ radians and advance the phase of the light in the $-\theta$ beam by ϕ radians, then the field incident at any point (x,y) is

$$a\, e^{i[\omega t-(\phi + \alpha x)]} + a.e^{i[\omega t + (\phi + \alpha x)]} = 2\, a\, e^{i\omega t} \text{ Cos } (\alpha x + \phi) \ldots (5)$$

Thus we see that the phase change in the incident light causes a phase change i.e., shift in the distribution of amplitude in the x,y plane. Conversely, if the x,y plane contains a transparency with transmission coefficient 2Cosαx and, if the mask is illuminated perpendicularly with parallel coherent monochromatic light, then the effect of moving the mask in the $\pm$ x direction is to change the phase

of the light diffracted into directions $\pm\theta$. If this light is focussed as in Fig 2.11 the magnitude of the amplitude at point R remains unchanged when the mask is moved in the $\pm$ x direction, but the phase at R depends on how much the mask is shifted in the x direction. Of course the mask must remain within the field of view of the lens and within the collimated beam of light.

2.4 NEED FOR COHERENT SYSTEM

Often one wonders what difference in the imaging system does it make when coherent and incoherent light sources are used. We make comparison in this section.

The Fourier transform relationship does not exist for the in-coherent case and so correlation cannot be achieved by this means. An example of a particular type of incoherent correlator is shown in Fig 2.12. The diffuse light source at the focal plane of the first lens spreads the beam at various angles with respect to the optic axis. The intensity at the image point is the product of transmission of the object transparency and displaced template transparency. The overlap of these two transparencies at different degrees of displacement is represented by separate image point intensities, so that the intensity distribution on the screen is the direct correlation of the object and template intensities.

For the coherent source the output intensity distribution be $I(x_i,y_i)$ when a spatially distributed source $g(x_0,y_0,t)$ is applied as an input to the imaging system. The output intensity distribution is

$$I(x_i,y_i) = | g(x_i,y_i) \otimes h(x_i,y_i)|^2 \quad \ldots\ldots\ldots\ldots\ldots\ldots (6)$$

When the distributed source is spatially incoherent then the output intensity is given by

$$I(x_i, y_i) = \langle u, u^* \rangle$$

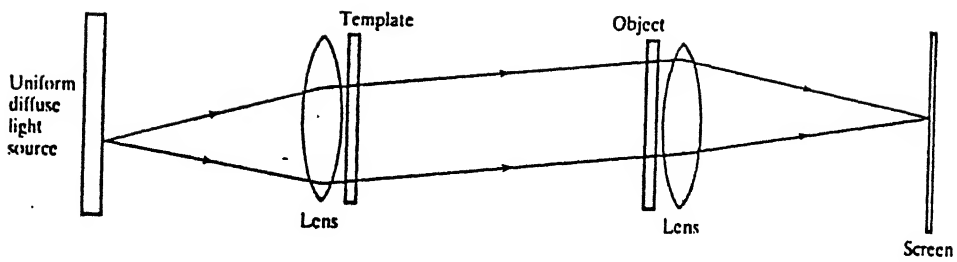

FIG 2.12 DIAGRAM OF INCOHERENT CORRELATOR

where u = light amplitude on the output plane

u^* = Complex conjucate of u

$\langle\ \rangle$ = operation of averaging in time.

$$I(x_i, y_i) = | g(x_i, y_i) |^2 \otimes | h(x_i, y_i) |^2 \quad \ldots\ldots\ldots\ldots\ldots\ldots (7)$$

The difference between (6) and (7) for coherent and incoherent light is the order in which the square modulus and convolution occur. For coherent light, the intensity is the square modulus of the convolution between the input function and the impulse response function, whereas for incoherent light, the intensity is the convolution between the square modulus of the input function and the square modulus of the impulse function.

The coherent systems perform correlation according to the principle of multiplication of the Fourier transforms of object and template amplitude/phase distributions and the subsequent Fourier transformation of the product when the input is in the form of a transparency an amplitude distribution is implied. Optical pattern recognition using incoherent light cannot utilize the phase

information of the image and the sensitivity is then smaller than that achieved using coherent light, but the input requirements are less stringent. With incoherent light, it is not necessary to ensure optical flatness of the input The number of data points that can be processed by incoherent method is about 10^4 [8] compared to the figure of 10^6 for a coherent system. The limitation is due to diffraction at the input device. Incoherent systems depend on the rectilinear propagation of light and this will only pertain to a relatively coarse mesh of data points. In contrast, the Fourier transform in coherent system is generated by diffraction and the development of high resolution input images to enhance diffraction effect.

2.5 FOURIER TRANSFORM PROPERTY OF LENS

One of the most remarkable and useful properties of a converging lens is its ability to perform two-dimensional Fourier transformation. The Fourier transforming operation is one with which we generally associate bulky, complex and expensive electronic spectrum analysers yet this complicated analog operation can be performed with extreme simplicity in a coherent optical system.

There are three separate configurations for performing the transform operation. In all the configurations the illumination is assumed monochromatic and the distribution of light amplitude across the back focal plane of the lens is of concern.In case of (a) the object to be transformed is placed directly against the lens itself. In the case of (b) the object is placed a distance d_f infront of the lens. In the case (c) the object is placed behind the lens at a distance d_f from the focal plane. All the three above mentioned configurations are shown in Fig 2.13.

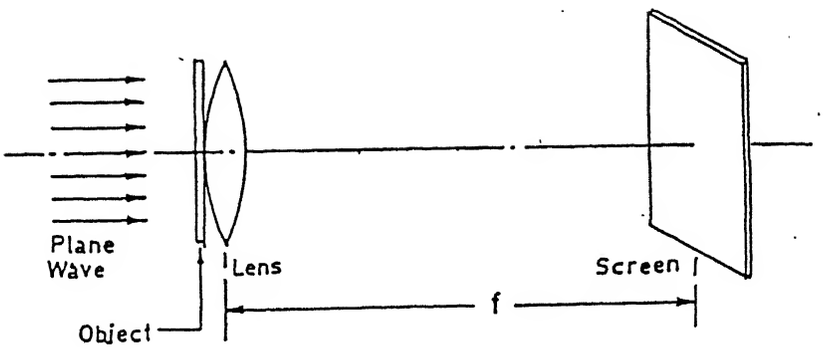

FIG 2.13 (a)

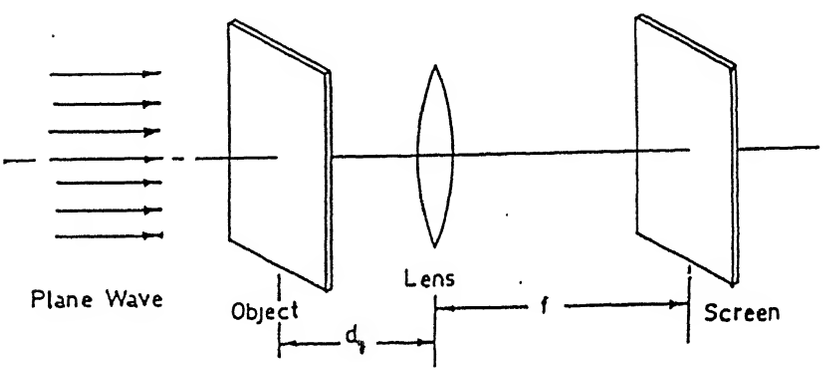

FIG 2.13 (b)

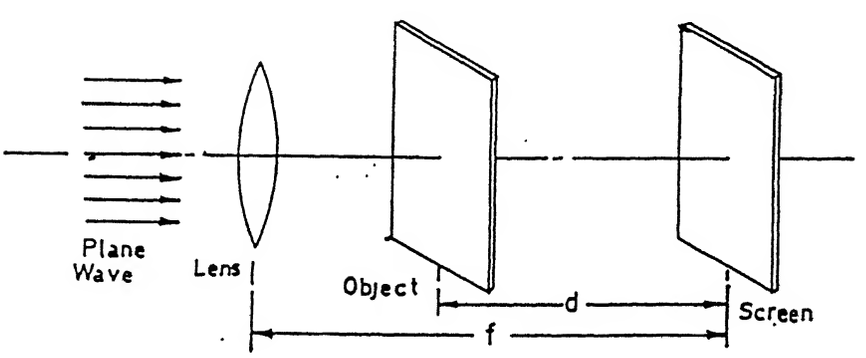

FIG 2.13 (c)

FIG 2.13 FOURIER TRANSFORMING CONFIGURATIONS
(a) OBJECT PLACED AGAINST THE LENS
(b) OBJECT PLACED INFRONT OF THE LENS
(c) OBJECT PLACED BEHIND THE LENS

Among all the three configurations case (b) is preferred where the object is placed in front of the lens at a distance equal to the focal length of the lens. This gives the exact Fourier transform relation cancelling the phase contribution arising from the difference between phase distribution across the object and focal plane. This can be seen in the following.

An input function $g(x_0,y_0)$ is located at a distance d_1 infront of the lens and the screen is at the back focal plane. The propagation distance is separated into two.

1. Propagation from the object to the lens and
2. Propagation from the lens to the screen.

The field distribution $g'(x,y)$ of the input function $g(x_0,y_0)$ which has propagated to the front surface of the lens is

$$g'(x,y) = g(x,y) \otimes fd_1 \qquad \ldots\ldots\ldots\ldots\ldots\ldots\ldots\ldots(8)$$

where $$fd_1 = \frac{1}{J\lambda d_1} \exp jk \left\{ \left[d_1 + \frac{(x^2+y^2)}{2d_1} \right] \right\} \qquad \ldots\ldots\ldots\ldots\ldots(9)$$

Here fd_1 represents point-source transfer function.

$$F\left[fd_1 \right] = F\, d_1(f_x,f_y) = \exp\left[jkd_1 - j\pi\lambda d_1 (f_x^2 + f_y^2) \right] \qquad \ldots\ldots\ldots(10)$$

The pattern at the back focal plane can be given as

$$E(x_i,y_i,f) = \frac{1}{j\lambda f} \exp\left[jk \left[f + \frac{x_i^2 + y_i^2}{2f} \right] \right] G'\left[\frac{x_i}{\lambda f}, \frac{y_i}{\lambda f} \right] \ldots(11)$$

$$\text{where } G'(f_x,f_y) = F\left[g'(x,y) \right] = G(f_x,f_y).\ F_{d1}(f_x,f_y) \ldots\ldots\ldots(12)$$

substituting (10) into (12) gives

$$E(x_i, y_i, f) = \frac{1}{j\lambda f} \exp\left[jk \left(d_1 + f + \frac{x_i^2 + y_i^2}{2f} \right) \right] G\left[\frac{x_i}{\lambda f}, \frac{y_i}{\lambda f} \right]$$

$$\exp\left\{ -j\pi\lambda d_1 \left[\left(\frac{x_i}{\lambda f} \right)^2 + \left(\frac{y_i}{\lambda f} \right)^2 \right] \right\} \quad \ldots\ldots\ldots(13)$$

$$= \frac{1}{j\lambda f} e^{jk(f + d_1)} \exp\left[jk \left(\frac{x_i^2 + y_i^2}{2f} \right) \left(1 - \frac{d_1}{f} \right) \right]$$

$$G\left[\frac{x_i}{\lambda f}, \frac{y_i}{\lambda f} \right]$$

when the input image is placed at the focal plane (d_1=f) the second exponential factor becomes unity and

$$E(x_i, y_i, f) = \frac{e^{j2kf}}{j\lambda f} G\left(\frac{x_i}{\lambda f}, \frac{y_i}{\lambda f} \right) \ldots\ldots\ldots(14)$$

Thus, the field distribution $G(x_i/\lambda f, y_i/\lambda f)$ on the screen becomes exactly the Fourier transform of the input function $g(x_0, y_0)$ if the input function is moved to the front focal plane and the screen is located at the back focal plane. The intensity distribution in the focal plane is the spatial frequency power spectrum.

2.6 PROPERTIES OF THE FRAUNHOFER DIFFRACTION PATTERN

When a film of two dimensional pattern whose light transmission function f(x,y) is inserted in the input plane, the Fourier transform F(u,v) of f(x,y) is obtained by the lens L_1 on the Fourier plane P_1 which is given by

$$F(u,v) = f(x,y).\exp -j(ux + vy)dxdy \quad \ldots\ldots\ldots(15)$$

The photodetector senses only intensity and therefore acts on the Fourier transform F(u,v) to give the energy density spectrum I(u,v), that is

$$I(u,v) = F(u,v)\ F(u,v)^{*} = |F(u,v)|^{2} \quad \ldots\ldots\ldots\ldots (16)$$

where * denotes complex conjugate.

The operation of obtaining I(u,v) from f(x,y) is defined as

$$I(u,v) = A\ (f(x,y))$$

Now some important properties of the operation A(.) in relation to pattern recognition is shown below.

PROPERTY 1

Energy density spectrum I(u,v) is invariant independently of the translation of a given pattern f(x,y). Let α,β be real constants, then this property is represented as

$$I(u,v) = A(f(x-\alpha\ ,y-\beta)) = A\ (f(x,y))$$

PROPERTY 2

When a pattern f(x,y) is given as a real function I(u,v) is symmetrical with respect to the origin, that is

$$I(u,v) = I(-u,-v)$$

PROPERTY 3

When the size of an original pattern is magnified ξ times broadwise and η times lengthwise and that the amplitude is intensified α times, we can obtain the following property.

$$A(\alpha f(x/\xi\ .y/\eta)) = \alpha^{2}\xi^{2}\eta^{2}\ I(\xi u,\eta u)$$

PROPERTY 4

When an original pattern $f(\rho,\phi)$ is rotated through α ,energy density spectrum $I(r,\theta)$ is also rotated the same angle that is

$$A(f(\rho,\ \phi + \alpha\ )) = I\ (r,\ \theta + \alpha)$$

These properties play an important role for designing the spatial filters.

2.7 IMAGE FORMATION AND FOURIER TRANSFORMATION

The most familiar property of lenses is their ability to form images. The incident light is diffracted by the object and the diffraction pattern formed when this diffracted light is brought to focus in the image. This is illustrated in the Fig 2.14

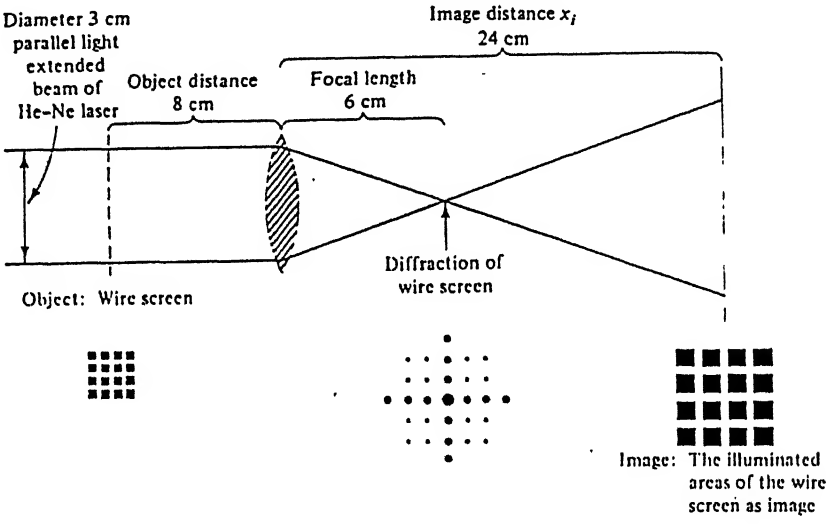

FIG 2.14 PROCESS OF IMAGE FORMATION

For the purpose of explanation, the process of diffraction and formation of the image can be considered as two separate steps but in actuality these are intimately connected. A small disturbance of the diffraction pattern may seriously change the image. To form an image all the waves scattered from one point x in the object have to be brought to a single point in space. Now the condition for an image point to exist is that all the waves should arrive at the point in the same phase, that is, that all the optical paths between the object and the image points should be equal. In the back focal plane of the lens all the waves that are parallel to each other will come to a focus; therefore in this plane the function $|\varphi^2|$ will be observed. Now since the relative phases between the object points O and image point I are the same and may be made zero. It is clear that the phase change between O and F is equal and opposite to the phase change between F

and I. Thus the relation between the wavefunction in the focal plane of the lens to that in the image is the inverse of that between the wave function in the object and that in the focal plane of the lens. In other words, the image is the inverse Fourier transform of φ (u)

$$f''(x) = \int \varphi(u) \exp(iku)\, du \qquad \text{.....(17)}$$

The Fourier transform property of the lens can be used to perform two Fourier transforms with two lenses to return to the original field distributions as shown in Fig 2.14 (a). To carry out simple imaging operations, it is not necessary,to have two lenses, the same can be demonstrated using single-lens as shown in Fig 2.14 (b).

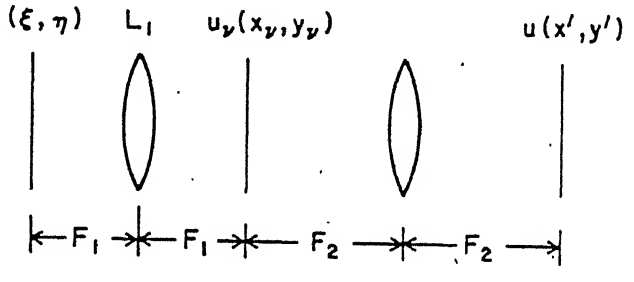

FIG 2.14 (a) A TWO-LENS IMAGING SYSTEM

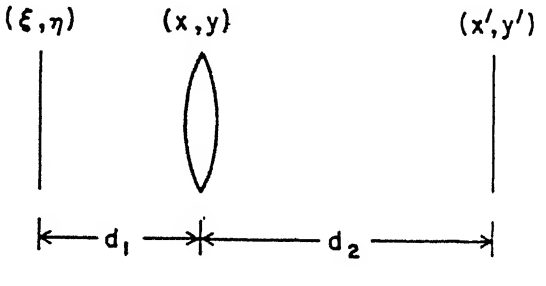

FIG 2.14 (b) A SINGLE LENS IMAGING SYSTEM

However, the image formed by a two-lens system differs from that formed by a single-lens system. Quadratic phase factors appearing in the two-lens system indicate the phase curvature over object and image planes.This can be eliminated by assuming that the light distribution at image point is contributed from a small region of the object space centered on its ideal geometrical object point..

The following Fig 2.15 illustrates the Fourier transformation of an object and Fourier transformation of Fourier transformation of the object resulting in object back. Fig 2.15 (a) shows athree-dimensional duck and Fig 2.15 (b) representes the three-dimensional Fourier transform of the duck. The Fourier trnasformhas aninverse relationship and hence one can mathematically calculate the three-dimensional transform from the three-dimensional duck structure. Fig 2.15 (c)isa two-dimensional structure which represents a projection of a 3-D duck. One can calculate 2-D Fourier transform from the 2-D projected picture likewise one can perform inverse operation also. Fig 2.15 (e) represents another "view " of the duck and Fig 2.15 (f) is the corresponding 2-D Fourier transform. From a sufficient number of 2-D Fourier transform which corresponds to different views of the structure, one may determine the 3-D Fourier transform of the structure. This can be inverse transformed to determine the 3-D structure.

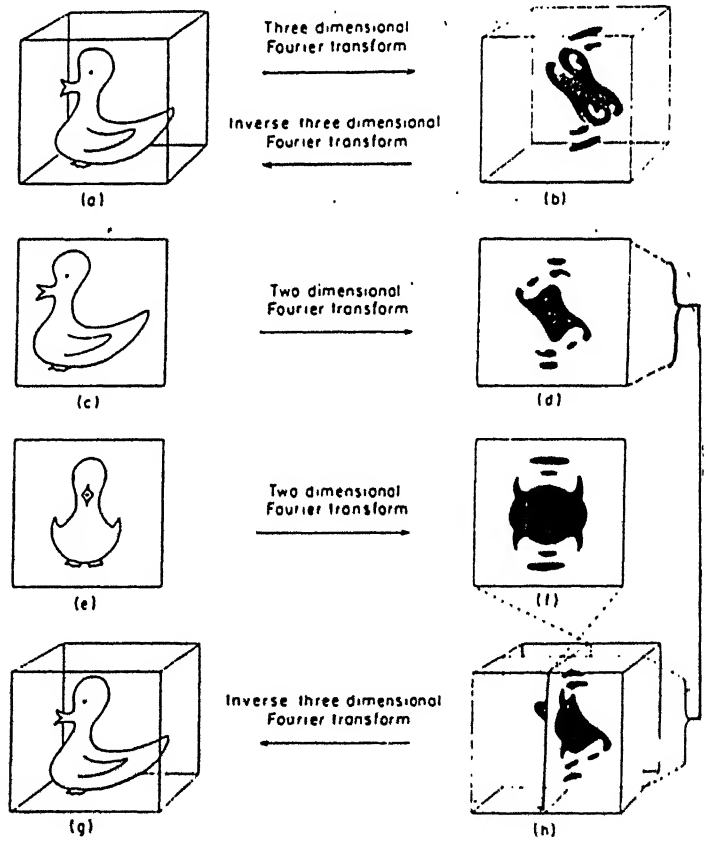

FIG 2.15 CONFIGURATION OF A THREE-DIMENSIONAL IMAGE FORMATION

2.8 SPATIAL FILTERING TECHNIQUE

A spatial filter can be thought of as the diffraction pattern of an object recorded on black and white photographic film. The developed film is the negative of the spatial filter that is desired, so it is contact printed or otherwise reversed to obtain the positive spatial filter.

When an object placed infront of the lens at a distance equal to the focal length of the lens is illuminated with monochromatic plane parallel light Fourier decomposed object is physically distinct in the focal plane of the lens. The field distribution in the focal plane is directly proportional to the object. If we insert a "filter" in the form of a thin,partially transmitting barrier at the focal plane, we can modify the Fourier transform of the object. In this way the final image may be modified. In mathematical terms

$$T(u,v) \text{ --------> } \tau_f(u,v)\ T(u,v) \quad \text{.....(18)}$$

so the image field distribution $E''_{\alpha}(x'',y'')$ is given by

$$E'_{\alpha}(x',y') = \left[\frac{A}{m}\right] \exp\left[i[\omega t - k(s+s')]\right] \exp\left[\frac{-i\,k\,r''}{2X}\right] \cdot$$

$$\int\int \tau_f(u,v)\ T(u,v)\ e^{i2\pi[u(x'/m) + v(y'/m)]}\ du\ dv \quad \text{....(19)}$$

The filter may simply block part of the Fourier plane thus eliminating some of the Fourier components in the reconstructed image.

To see how this works consider an example shown in Fig 2.16. If we block off all the spots except the ones belonging to the diffraction pattern of the vertical lines, the image shows only the

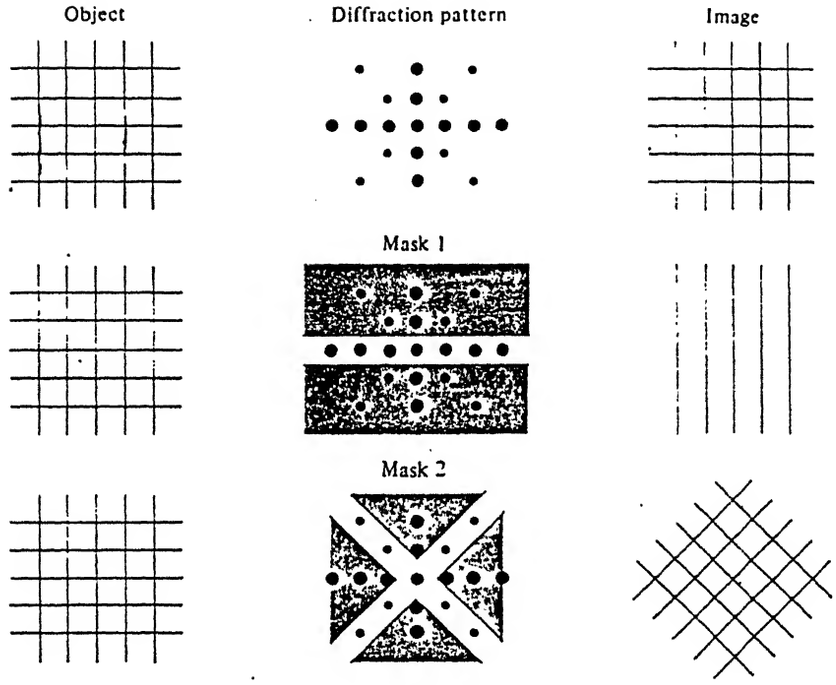

FIG 2.16 EFFECT OF SPATIAL FILTERING ON IMAGE

vertical lines. If we let pass only the spots on the diagonals at 45^{O}, we see a grid rotated by 45^{O} although such lines do not exist in the original object screen.

On the subject of spatial filtering let us consider a few simple spatial filters which provide visually, quite dramatic filtered results. Examples of simple filters which affect the amplitudes of object spectra are zero spatial frequency stop and a horizontal slit placed at the center of plane P_2. An example of a simple phase filter is one which retards the zero frequency component of the object spectrum by 90°.

When a filter of the zero spatial frequency stop is used, the average transmittance of an image will be eliminated yielding, the high pass filtered result of Fig 2.17 (b) from the original image of Fig 2.17 (a).

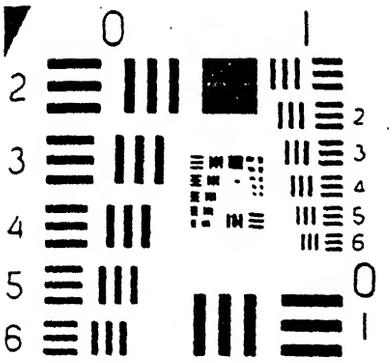

FIG 2.17 (a) ORIGINAL IMAGE

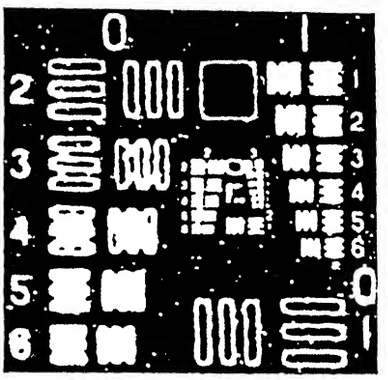

FIG 2.17 (b) HIGH-PASS FILTERED IMAGE

A 90° phase filter can help to visualize transparent objects. Let the amplitude transmittance of a transparent object be

$$f(\xi,\eta) = \exp [j\phi(\xi,\eta)]$$

and assume that the phase $\phi(\xi,\eta)$ be less than 1 radian such that

$$f(\xi,\eta) \cong 1 + j\phi(\xi,\eta)$$

When this spectrum of the transparent object is filtered by retarding the phase of its zero spatial frequency component by 90° relative to other frequency components, the intensity of the filtered image is

$$I(x",y") \cong 1 + 2\phi(x",y")$$

Thus the intensity variation is certainly visible.

The following Fig 2.18 shows the spatial filtering arrangement. Collimated beam coming from a point source illuminates the object which has complex amplitude distribution $T(\xi)$, produces by diffraction a complex amplitude distribution f(x) in the pupil of the lens L_2 where f(x) is the focal plane of the lens L_1, if the object itself was illuminated in collimated light as shown. In this case, the complex amplitude f(x) is equal to the Fourier transform of the complex

amplitude $T(\xi)$ in the object. The complex amplitude f(x) is frequently described as the complex diffraction pattern of the object.

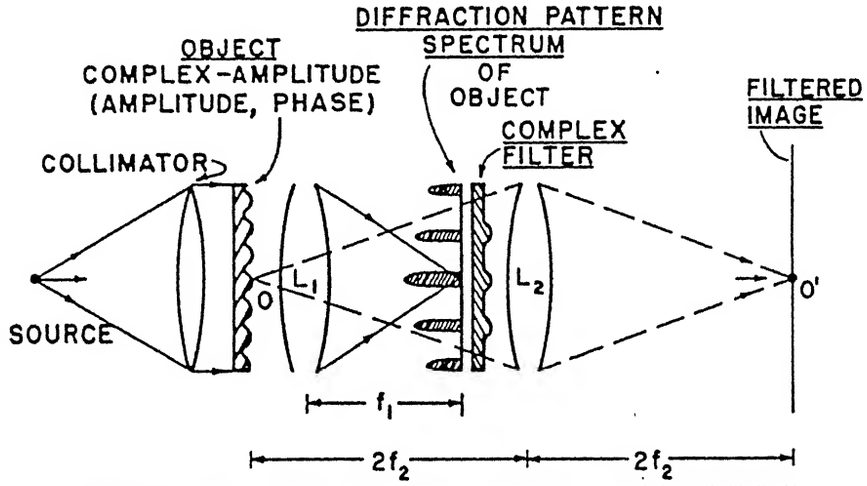

FIG 2.18 SPATIAL FILTERING ARRANGEMENT

The light arriving at the lens L_2 form an image in ξ'' plane and the image $T(\xi'')$ is obtained by second diffraction taking place by the field f(x) in the pupil of L_2. It is clear from the above Fig 2.18 that the image amplitude $T(\xi'')$ is obtained by the Fourier transformation of the amplitude f(x) and therefore the image amplitude $T(\xi'')$ will be equal to the object amplitude $T(\xi)$ if no complex filter is used next to f(x). The above arrangement is normally used for phase contrast filtering.

Another method used by Cutrona et..al for spatial filtering is shown below in Fig 2.19. This method is quite generally used for Correlation filtering.

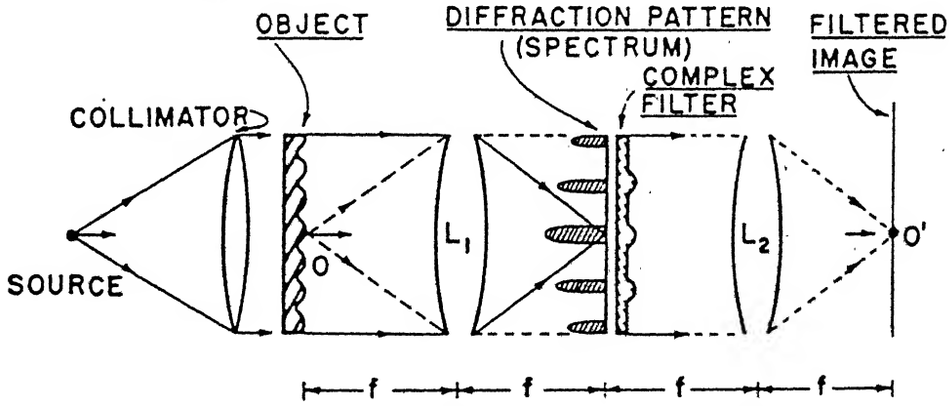

FIG 2.19 SPATIAL FILTERING ARRANGEMENT

CHAPTER 3

EXPERIMENTAL REQUIREMENTS AND PROCEDURE

3.1 INTRODUCTION

This chapter gives a brief outlay of various requirements and considerations given in selecting the components of the optical system and the procedure involved in obtaining Diffraction pattern of various fingerprints for the spatial filtering process.

3.2 SELECTION OF OPTICAL SYSTEM

3.2.1 NEED FOR LASER:

When an incoherent source such as white light illuminates a transparent periodic object, part of the light passing directly through the object gets focussed by the lens and form zeroth order diffraction pattern. Part of the light deviated to various angles on each side of the undeviated ray gets focused at different points, since it contains various colours. Hence a rainbow or spectrum rather than a simple point of white light appears [see Fig 3.1 (a) & (b)].

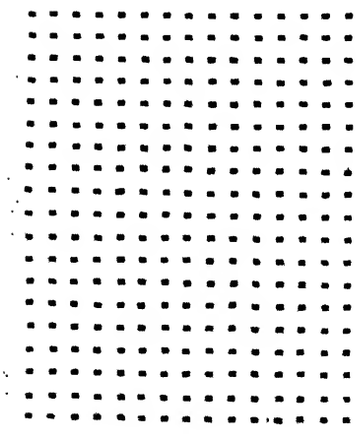

FIG 3.1 (a) OBJECT

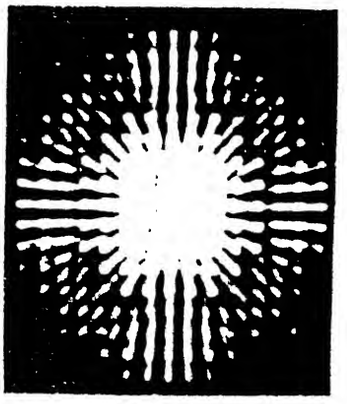

FIG 3.1 (b) ITS DIFFRACTION PATTERN

If a monochromatic source is used, the diffraction pattern will be a point rather than a spectrum. The diffraction order will extend infinitely on both sides of the zeroth order but successive orders will be less intense by an order of magnitude and so only few orders can be seen .[see Fig 3.1 (a) and Fig 3.1 (c)]

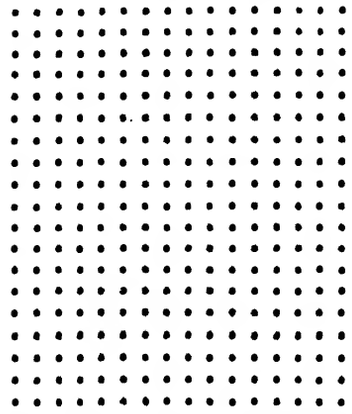

FIG 3.1 (a) OBJECT

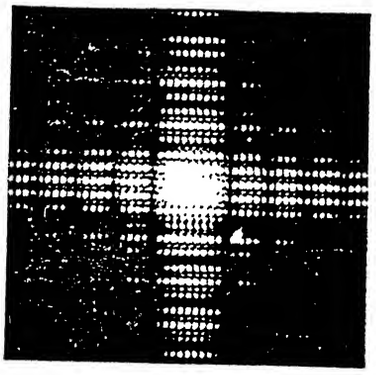

FIG 3.1 (c) ITS DIFFRACTION PATTERN

3.2.1.1 TEMPORAL COHERENCE:

The temporal coherence of the laser is the average duration of phase integrity of the light wave. It is commonly expressed by the linewidth of the radiation, broad linewidths are being associated with short temporal coherence.

The values of some typical multimode lasers are given below.

TABLE 2

LASER	$\frac{\Delta\lambda}{\lambda}$	Δl (cm)
He-Ne	3×10^{-6}	18
Ar^{+}	10^{-5}	5
AlGaAs	2×10^{-3}	0.03
Nd:YAG	4×10^{-5}	0.25

The above table shows that He-Ne is an ideal choice.

3.2.1.2. SPATIAL COHERENCE

The spatial coherence of an extended light beam refers to lateral phase integrity across the wavefront. If the laser beam is expanded with a pinhole and a collimator spatial coherence of the laser can be maintained.

3.2.1.3 POWER REQUIREMENT

The laser dissipates the largest fraction of the electrical power required to operate the correlator. Since one of the salient advantages of the optical correlator is the lower power dissipation, it is important to minimise this parameter to gain maximum advantage. Moreover to increase the image contrast a low power laser has to be used and so 5 mW He-Ne laser is chosen.

3.2.2 FOURIER TRANSFORM LENS

To satisfy the paraxial approximation for Fourier transform operation by a thin lens, the size of the lens aperture and the input object are frequently restricted. It is a desirable feature of a Fourier transform lens to be able to accept input objects of larger size, say sizes up to 75% of the lens. The accuracy of the Fourier transform depends both on the precision with which the input and Fourier plane recording devices can be located and the freedom from aberration of the lens system. The fractional error of location can be reduced if a long focal length lens is chosen. Moreover the size of a F.T pattern is proportional to the focal length,it would be desirable for the F.T lens to have a long focal length but short physical distance between the exit pupil and lens vortex. Furthermore, it would be desirable for the F.T plane to be flat.

3.2.3 PINHOLE CAMERA

To record the diffraction pattern of various fingerprints, a lenseless camera is used. This has the advantage of recording the exact size of the diffraction pattern, which is very essential in designing the spatial filter. The camera should have variable shutter speed for optimum exposure of the pattern.

3.2.4 RECORDING MATERIAL

Normally OR-WO panchromatic film made up of a thin, light sensitive emulsion on one side is used. The emulsion is a suspension of small silver-halide grains in gelatin. The grains are light sensitive in that they are rendered developable by exposure to light. Untreated silver-halide grains themselves are sensitive only to blue and ultraviolet parts of the spectrum as shown in Fig 3.2. Most films designed for pictorial use are panchromatic and respond to the entire visible spectrum.

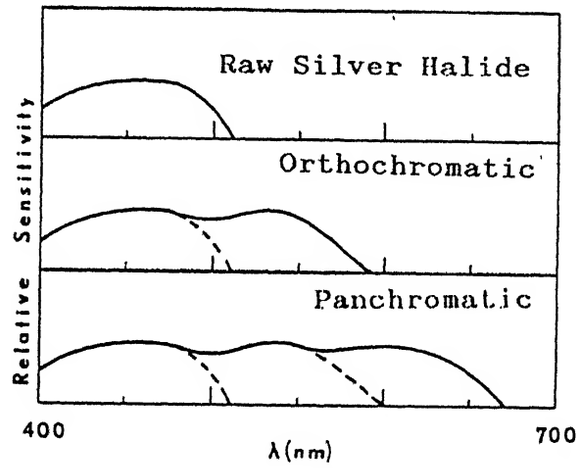

FIG 3.2 SPECTRAL SENSITIVITIES OF TYPICAL PHOTOGRAPHIC EMULSIONS

3.2.5 OPTICAL BENCH

The whole experiment has to be carried out on an Optical bench. This has provision for online arrangement of various optical components. This bench contains optical mounts which can be moved in X-Y directions and has provision for rotation along y-direction.

3.3 PROCEDURE

A beam of 5 mW He-Ne laser after expansion to about 3 cms is allowed to pass through the fingerprint recorded on a transparent material failed to show diffraction pattern on the screen. The plausible reason might be low angular diffraction of the plane waves passing through the transparency. The angle of diffraction θ is given by

$$\sin\theta = \left[\frac{m\lambda}{D}\right] \quad \ldots\ldots\ldots\ldots\ldots\ldots\ldots\ldots\ldots\ldots(20)$$

where

λ = wavelength of the monochromatic light

D = grating element

To increase θ either D should be decreased or λ should be increased. Increasing λ doesn t solve the purpose and hence the fingerprint pattern is compressed to few millimeters in a good quality high resolution Diazo film.

Fig 3.3 shows the schematic diagram of the experimental setup used for Fourier transform recording. A 5 mW He-Ne laser beam illuminates the input transparency which has the fingerprint pattern, located in the plane P_1. The input plane lies in the front focal plane of the converging F.T lens having focal length f. The F.T lens L_1 forms the F.T F(u,v) of the input image f(x,y) in its back focal plane p_2. The pinhole camera is placed in the focal plane P_2 and the F.T of the input image is recorded. A spatial filter is F.T of the object recorded on black and white photographic film. The developed film is the negative of the spatial filter that is desired, so it is contact printed or reversed to obtain the positive spatial filter. The spatial filter is merely a special variety of Hologram and as such, it is possible to transform the spatial filter and reconstruct the image of the original object.

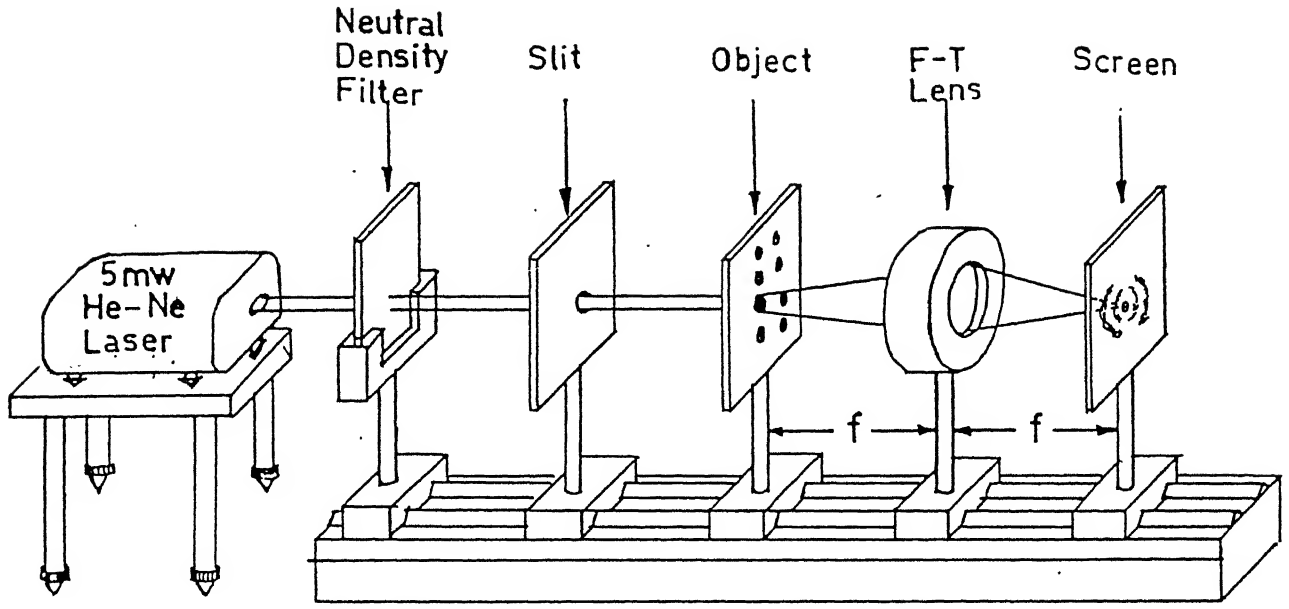

FIG 3.3 SCHEMATIC DIAGRAM OF FOURIER TRANSFORM RECORDING

SPATIAL FILTERING

3.3.1 FILTERING TECHNIQUE

Fig 3.4 depicts the coherent imaging system used for the recognition of fingerprints by matched filtering technique. A particular fingerprint g(x,y) is inserted at the focal plane of the F.T lens L_1. This lens produces the Fourier transform of the fingerprint $G(f_x, f_y)$ in its back focal plane P_2. In the plane P_2 spatial filter (obtained using the experimental arrangement of Fig 3.3) of various fingerprints are introduced one by one for examination. The transparent portion of the filter transmits some of the spatial frequencies, while the opaque part completely blocks all other spatial frequencies. The focussing lens then reconstructs the diffraction pattern but only where the light is transmitted. A pinhole camera is placed in the plane P_3 and the image formed by the lens L_2 for the introduction of filters are photographed. The same process is repeated with various fingerprints inserted in the plane P_2.

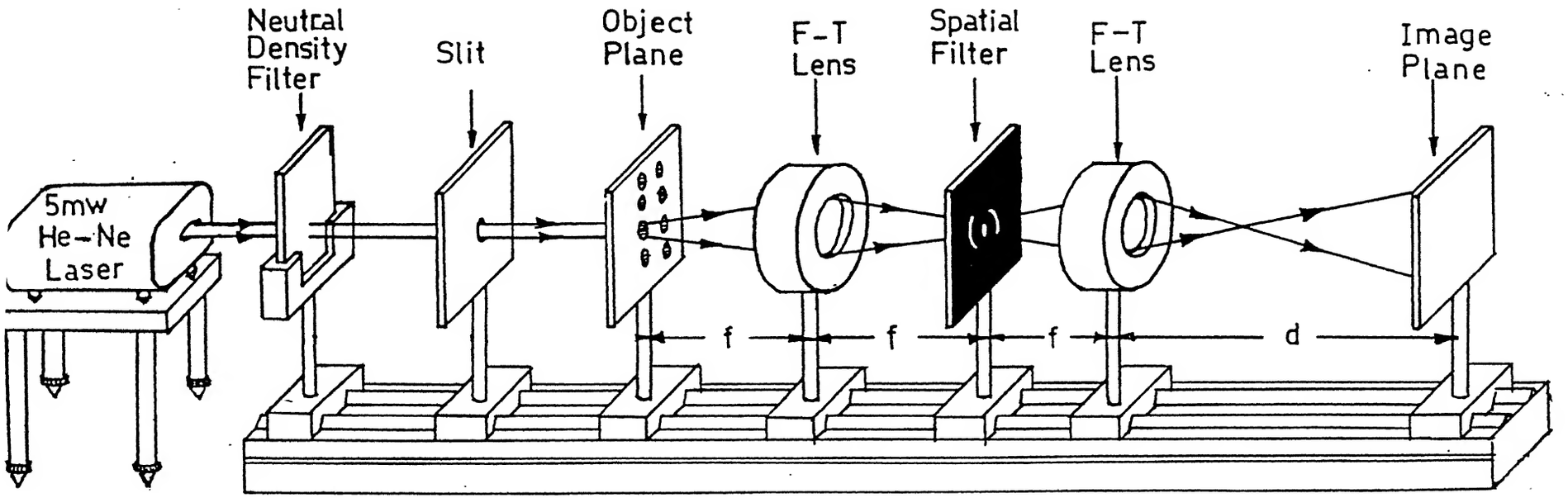

FIG 3.4 SCHEMATIC DIAGRAM OF THE SPATIAL FILTERING ARRANGEMENT

Practical difficulties:

The light transmitted by the spatial filter during recognition process contains not only the image of the fingerprints but several other components are also present. These unwanted components produce ghost images which are superimposed on the recognised image causing the desired image pattern to become unintelligible by reducing the contrast of the image. Moreover little difference in the magnitude of light transmitted by the filter contribute subtle changes in the quality of the image. These changes cannot be observed by naked eye causing recognition process to be rather difficult.

These problems have been surmounted to a great extent by using ϕ-Fourier method of pattern recognition.

3.3.2 ϕ-FOURIER METHOD

ϕ-Fourier method composed of an optical system is shown in Fig 3.5. A film of a two-dimensional fingerprint pattern whose light transmission function is $f(x,y)$ is inserted into the input plane P_1. The Fourier transform $F(u,v)$ of the fingerprint pattern is formed by the foucssing lens L_1 on the Fraunhofer image plane P_2. In that plane P_2 various spatial filters recorded using the experimental set-up (Fig 3.3) areintroduced .The spatial filter modifies light amplitude transmittance and the spatial frequencies which are transmitted by the transparent portions of the filter are focussed by the lens L_2 on to the photodetector which is kept at its focal plane of L_2. If the Fourier Transform of the object introduced at the input plane P_1 matches with the transparent portion of the filter then all the spatial frequencies will be transmitted and the detector output shows maximum value. When different unmatched filters are introduced in the plane P_2 , the light transmitted by the filter decreases correspondingly depending on the amount of higher spatial frequencies

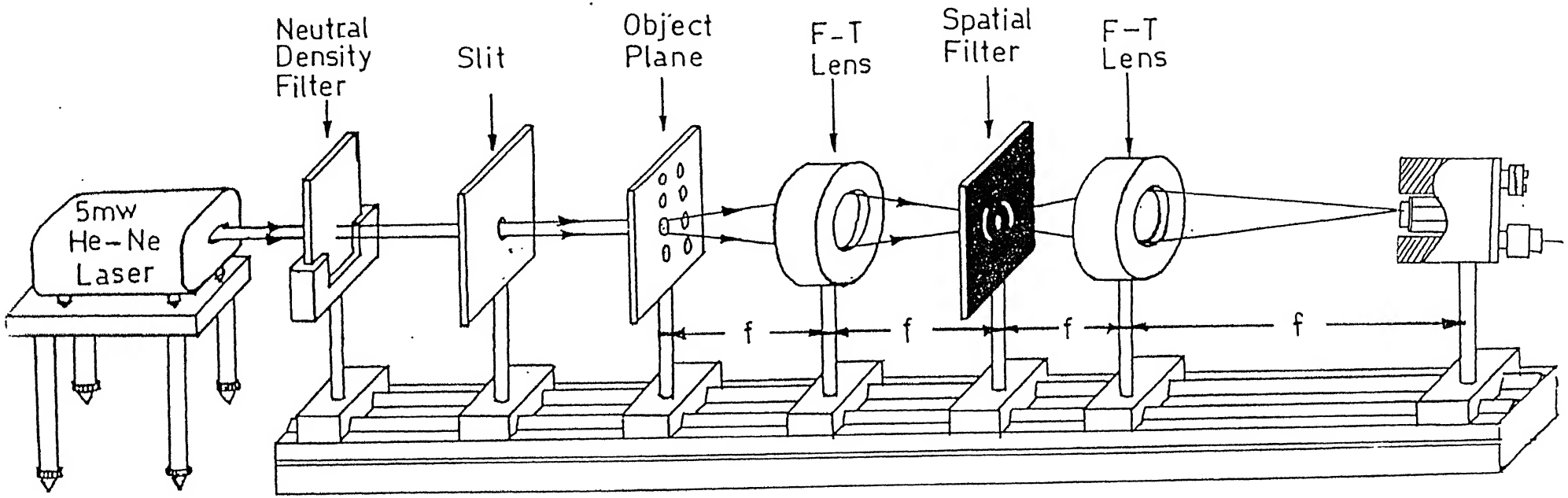

FIG 3.5 OPTICAL ARRANGEMENT USED FOR 4-FOURIER METHOD

blocked and the photodetector records different values. The same process is repeated for various fingerprints introduced at the input plane P_1. From the value of the photodetector output the shape searched can be identified.

CHAPTER 4

RESULTS AND DISCUSSION

4.1 INTRODUCTION

The Fourier spectra of various fingerprint patterns obtained using Coherent Optical Processing system of Fig 3.3 are depicted below in section 4.2 followed by some discussion .

Keeping various filters in the filtering plane P_2 the results obtained in the image plane using Matched Filtering Technique are shown in Fig 4.13. The θ-Fourier method is discussed at the end of this chapter and the results obtained are tabulated in Table 3.

4.2 FOURIER TRANSFORM OF FINGERPRINTS

From Figures 4.1 to 4.6 it is clear that although each fingerprint has a unique spatial frequency spectral signature they have certain features in common based on their structures. Since the predominant ridge patterns are periodic, with small variations in period, the frequency spectra are characterised by circular bands of spatial frequencies whose extent follow from the basic ridge orientations in the print.

Fig 4.1 (a) shows the Fourier spectra of fingerprint specimen (A). This indicates a ring with gaps on the sides. This is due to the fact that most of the ridges in the Fig 4.1 are horizontally positioned with very few of them oriented vertically. Hence major contribution to the Fourier spectra comes only from the horizontal ridges.

The specimen (B) shown below in Fig 4.2 is called Central Pocket loop. This figure is characterised by the fact that majority of the ridges are running horizontal in the middle and hence the frequency spectra is concentrated in top and bottom portion of the circle lying next to the central spot. In the beginning as well as in the end of the fingerprint pattern the ridges have bent downwards in the top portion and upwards in the bottom portion. This bent ridges give little frequency spectra on the sides thereby filling up the side gaps [See Fig 4.2 (a)] and a circular loop like structure lying in the

FINGERPRINT
SPECIMEN A

FIG 4.1

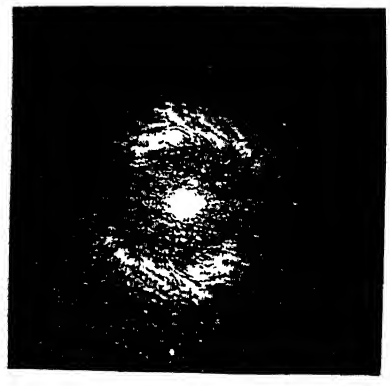

ITS FOURIER
TRANSFORM

FIG 4.1 (a)

FINGERPRINT
SPECIMEN B

FIG 4.2

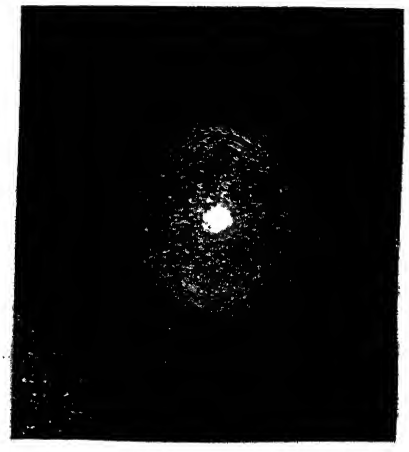

ITS FOURIER
TRANSFORM

FIG 4.2 (a)

middle of Fig 4.2 contributes equal spectra on all the sides thereby again filling some of the gaps left on the sides. A close observation of the Fig 4.2 reveals that the ridge spacing is quite less compared to the ridge spacing of Fig 4.1 and hence the higher frequency spectra of Fig 4.2 (a) are well sepaprated from the central spot.

In Fig 4.3 almost all the ridges are circularly oriented and the central ridge is also exactly circular in shape and hence the name

FINGERPRINT
SPECIMEN C

FIG 4.3

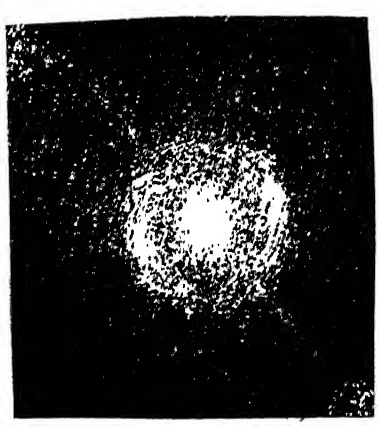

ITS FOURIER
TRANSFORM

FIG 4.3 (a)

Plain whorl. These ridges contributes equal spatial frequency spectra on all the sides. A close observation of Fig 4.3 (a) disclose the fact that the concentration of frequency spectra is more on the sides rather than on top and bottom portions of the circle. This may be due to predominant vertical orientation of the ridges. As a whole the Fourier transform of Fig 4.3 looks like an Airy disc as shown in Fig 4.3 (a).

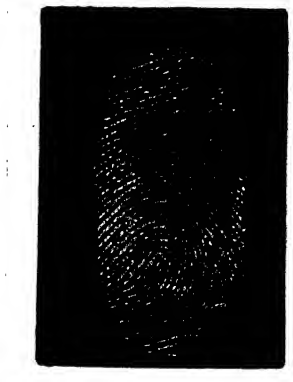

FINGERPRINT
SPECIMEN D

FIG 4.4

ITS FOURIER
TRANSFORM

FIG 4.4 (a)

Fig 4.4 looks like the mirror image of Fig 4.1. This is because both the fingerprints are of the same person. The previous figure (Fig 4.1) showing the impression of his right thumb and latter one of his left thumb. The difference lies only in the orientation of the pattern. This subtle difference is best reflected in their Fourier spectra [See Fig 4.1 (a) and Fig 4.4 (a)]. These type of patterns can be best distinguished from their Fourier spectra. Here we would like to issue a warning that not all the left and right hand thumb impressions are mirror images of each other. Investigation carried out in this regard reveals that the left and right hand impressions of the some persons are entirely different [See Figs 4.6 (a) and (b)].

The Fourier spectra of Fig 4.5 looks almost circular in shape. This is because the central loop is somewhat circular in shape and most of the ridges on the sides are spirally bent. Fig 4.5 (a) looks very similar to that of Fig 4.3 (a). The only difference being that the concentration of the Fourier spectra now moved to a different place in the outer circle.

FINGERPRINT
SPECIMEN E

FIG 4.5

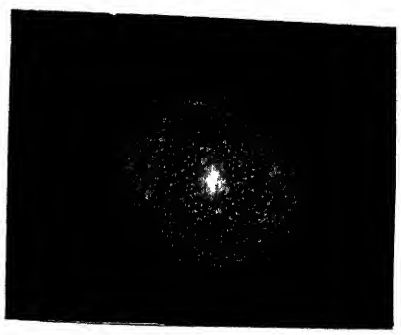

ITS FOURIER
TRANSFORM

FIG 4.5 (a)

FINGERPRINT
SPECIMEN F

FIG 4.6 (a)

FINGERPRINT
SPECIMEN G

FIG 4.6 (b)

Depending upon the kind of ridge patterns the spatial frequency spectra move around the sides of the circular loop. It is also clear from the Figures 4.1 to 4.6 that most fingerprints are binary in nature and hence harmonic energy visible in the Fourier Spectra shows rings of larger radii as noise.This arises due to Silver-halide grains of the photographic film, presence of dust particles in the film and coherence of the laser source itself. These are called laser speckle.

Before considering the details of Matched filtering technique it

is worthwhile to consider the effect of High-pass and Low-pass filters on the image quality.

4.3 FABRICATION OF FILTERS

A low-pass filter can be fabricated on a film by exposing the film to lower spatial frequencies (central spot) of the fingerprint, blocking all the higher spatial frequencies. The developed film is contact printed or reversed to obtain a positive spatial filter. Similarly a high-pass filter can be fabricated by exposing the film to the higher spatial frequencies of the fingerprint, blocking the central spot and contact printing the developed film. Fig 4.7 and Fig 4.8 show the low-pass and high-pass filters fabricated by us.

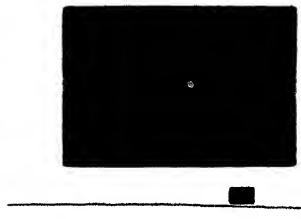

LOW-PASS FILTER

FIG 4.7

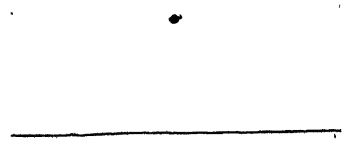

HIGH-PASS FILTER

FIG 4.8

Fig 4.9 (a) is the object whose transparency is placed in the plane P_1 of Fig 3.4 and the image formed in the plane P_3 is photographed and it is shown in Fig 4.9 (b). Then a low pass filter shown above (See Fig 4.7) is introduced in the plane P_2. The light transmitted by the filter is reconstructed by the lens L_2 and it forms an image in the plane P_3. The pinhole camera is placed in the plane P_3 and the image formed is photographed. Fig 4.9 (c) shows the image obtained in the plane P_3 with the introduction of low pass filter.

It is obvious from this figure that a low-pass filter gives only the shape of the fingerprint and details of the ridge pattern are missing. The low-pass filter blocked all the higher spatial frequencies which can give complete information about the ridge patterns and so the image detail is completely wiped out.

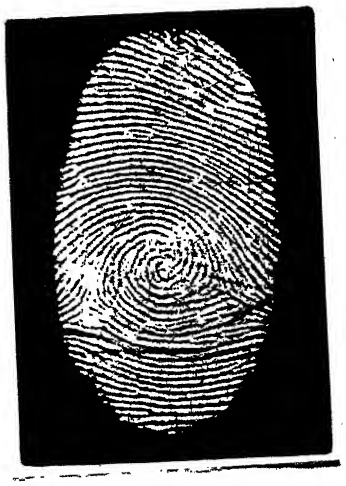

OBJECT
SPECIMEN A

FIG 4.9 (a)

IMAGE OF
SPECIMEN A

FIG 4.9 (b)

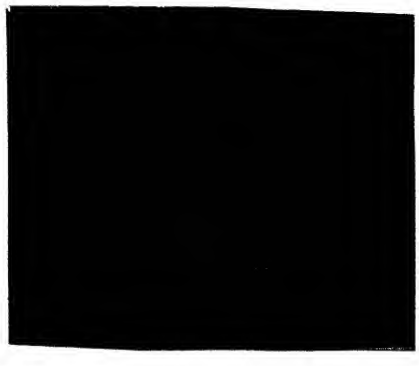

LOW-PASS FIL-
TERED IMAGE

FIG 4.9 (c)

The process adopted above for recording the low-pass filtered image is repeated for the high-pass filter and the resultant image formed is shown below in Fig 4.10.

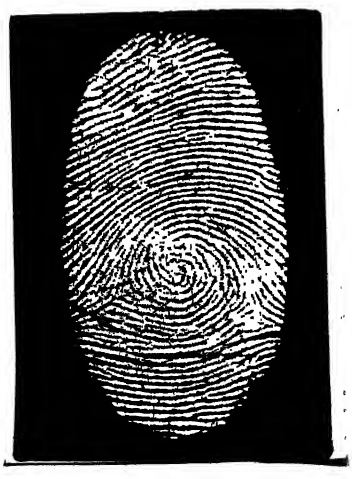

OBJECT
SPECIMEN A

FIG 4.10 (a)

IMAGE OF
SPECIMEN A

FIG 4.10 (b)

HIGH-PASS FIL-
TERED IMAGE

FIG 4.10 (c)

The image shows some details of the ridge pattern along with the shape of the fingerprint pattern. The higher spatial frequencies contain much of the information about the object and image formed can be seen only at one particular distance. The image formed is less distinct due to absence of lower spatial frequencies.

Eventhough the Fourier transform of the fingerprint formed on the plane P_2 and the filter inserted in the same plane matches quite well, the output image is not clear due to speckle effect. Contributions to the speckle effect comes from grains in the photographic film and coherence of the laser. This speckle effect arises mainly due to higher spatial frequencies and so if a low-pass filter capable of blocking all the higher spatial frequencies of the speckle but to pass both low and high spatial frequency contributions of the fingerprint is synthesized and inserted in the plane P_2, then quality of the image will improve considerably. A filter to remove the speckle effect can be prepared by exposing the film to lower and higher spatial frequency components of the fingerprints blocking all the higher frequency contributions of the speckle. The developed film is reversed or contact printed to obtain the positive spatial filter. Figure 4.11 shows the filter prepared to remove the speckle effect. Figure 4.11 (b), (c), (d) and (e) depict the quality of image obtained with and without the introduction of filter.

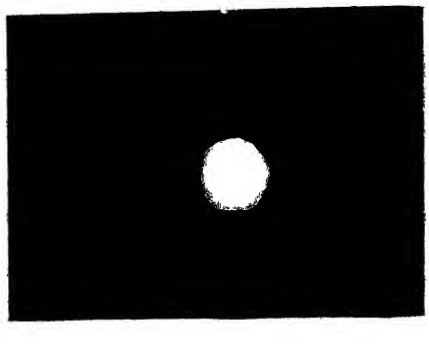

HIGH-PASS FILTER TO REMOVE SPECKLE EFFECT

FIG 4.11

OBJECT
SPECIMEN A

FIG 4.11 (a)

ITS IMAGE WITH
WITH SPECKLE

FIG 4.11 (b)

ITS IMAGE WITH-
OUT SPECKLE

FIG 4.11 (c)

HIGH-PASS FILTERED IMAGE
WITH SPECKLE

FIG 4.11 (d)

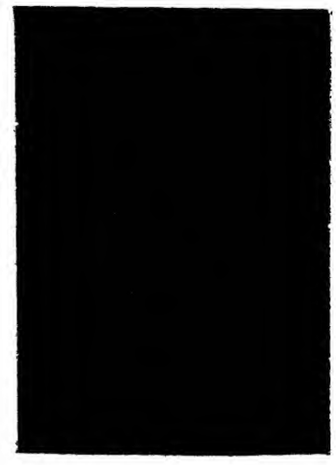

HIGH-PASS FILTERED IMAGE
WITHOUT SPECKLE

FIG 4.11 (e)

4.4 FILTERING TECHNIQUE

In the Figure 3.4 if the spatial filter $G^*(f_x,f_y)$ introduced in the plane P_2 is matched with $G(f_x,f_y)$ the filter passes all the spatial frequencies. The light transmitted through the spatial filter is given by

$$G(f_x,f_y)\, e^{j\phi(f_x,f_y)}\; C(f_x,f_y)\, e^{-j\phi(f_x,f_y)} \quad \text{.....(21)}$$

The first term denotes the Fourier transform of the input and the second term signifies the transmittance of the spatial filter. When the amplitude distribution of the input matches with that of the transmittance of the spatial filter the output becomes maximum. The phase factor in the equation (21) becomes zero throughout the filter and the distribution beyond the filter becomes a parallel beam so that all the output from the lens L_2 forms an image which has one-to-one correspondence with the object [see Fig 4.12 (a) and (b)]. The filter used to obtain the image is also shown below [see Fig 4.12 (c)]

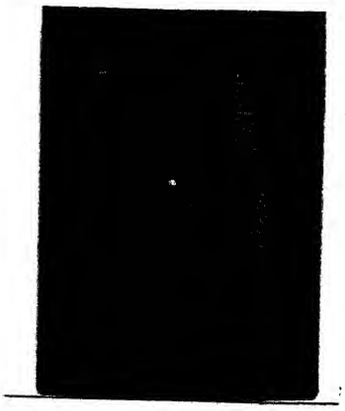

OBJECT

FIG 4.12 (a)

ITS FILTER IMAGE

FIG 4.12 (b)

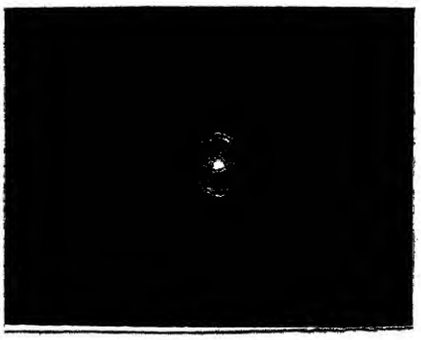

FILTER

FIG 4.12 (c)

In case of most fingerprints the low spatial frequency components remain invariant but higher spatial frequencies move around a circle

depending on the orientation of the ridge pattern. In case the filter $G''^{*}(f_x, f_y)$ and the Fourier transform of the object (fingerprint) are different then some of the higher spatial frequencies get blocked . So the light transmitted by the filter decreases correspondingly and

IMAGE OBTAINED USING . FOR VARIOUS FILTERS

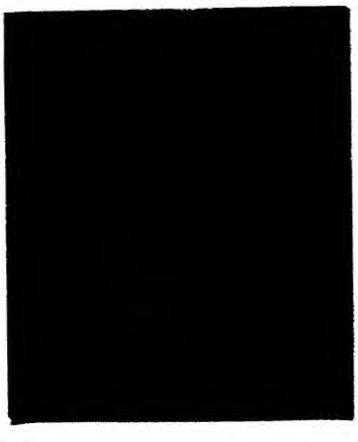

WITH FILTER A

FIG 4.13 (a)

WITH FILTER B

FIG 4.13 (b)

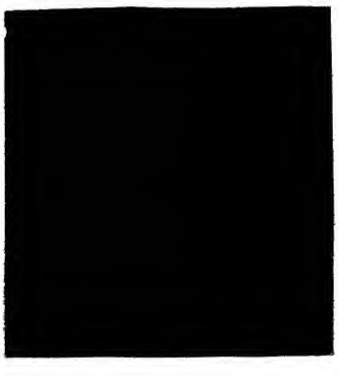

WITH FILTER C

FIG 4.13 (c)

WITH FILTER D

FIG 4.13 (d)

WITH FILTER E

FIG 4.13 (e)

FIG 4.13 RECOGNITION OF ONE FINGERPRINT IN A GROUP OF FIVE SIMILAR FINGERPRINTS. *FIG B SHOWS THE RECOGNITION* WHILE THE REMAINING FOUR SHOWS ONLY DISTORTED IMAGE

the phase factor of equation (21) remains non-zero. The image formed at the plane P_3 not only becomes blurred but distortions are also introduced due to blocking of some of the higher spatial frequencies of the object by the filter introduced at P_2. By observing the quality of the image formed at the plane P_3 (See Fig 4.13) one can recognise the pattern looking for.

FIG 4.14 VARIOUS FILTERS USED IN THE FILTERING TECHNIQUE

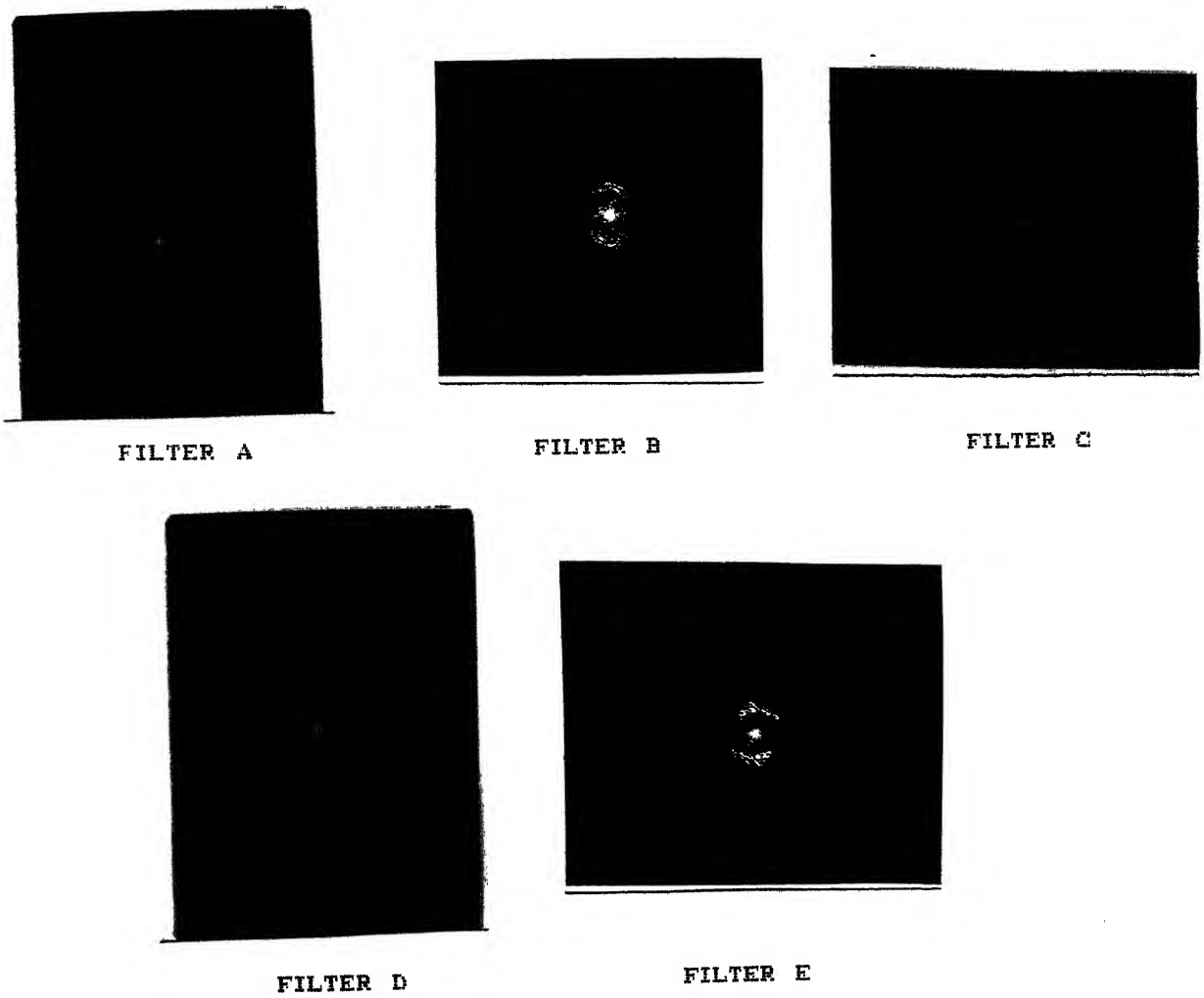

FILTER A FILTER B FILTER C

FILTER D FILTER E

4.5 Θ-FOURIER METHOD

In this method, instead of visualising the image contributed by the light transmitted by the filter on the plane P_3, a photodetector

is kept at the focal plane of the lens L_2. When the Fourier transform of the fingerprint introduced at P_1 and the filter $G^*(f_x,f_y)$ inserted in the plane P_2 matches then the light transmitted by the transparent portion of the filter is maximum and the detector shows high output. When filter of any other distribution is used in the plane P_2 some of the higher spatial frequencies get eliminated and the photodetector output decreases correspondingly. The process is repeated for different fingerprints and the detector output is noted. From the detector output one can identify the pattern searching for. Table 3 shows the detector output noted using the above method.

TABLE 3

S.No.	FINGERPRINT	SPATIAL FILTER	DETECTOR OUTPUT (in volts)
1	A	A	0.2425
2	A	B	0.2350
3	A	C	0.2375
4	A	D	0.2375
5	A	E	0.2400
6	B	A	0.310
7	B	B	0.320
8	B	C	0.315
9	B	D	0.315
10	B	E	0.316
11	C	A	0.320
12	C	B	0.321
13	C	C	0.323
14	C	D	0.321
15	C	E	0.321

16	E	A	0.321
17	C	B	0.322
18	B	C	0.321
19	A	D	0.325
20	D	E	0.320

Depending on the amount of light transmitted by the filter the detector output varies. The output values shown in Table 3 indicates that when the object pattern introduced at the plane P_1 and the filter introduced at the plane P_2 of Fig 3.5 matches then the detector output goes to maximum. For unmatched filters the output decreases to a value corresponding to the amount of spatial frequencies blocked by the filter. In some cases the output values remain the same for different filters. This is due to the fact that the detector is unable to detect subtle difference in the amount of light transmitted by the filter.

Now again consider the detector output values shown in Table 3 for various fingerprint specimens A, B, C and D when different filters were introduced in the filtering plane. It is obvious that even for the matched filter the detector output varies from one type of fingerprint specimen to another. This is due to the fact that the ridge pattern and the transmission coefficient of the film varies for different fingerprints.

Now considering one particular type of fingerprint pattern say B, let us analyse the reason for variation in the detector output.

When the positive spatial filter of the object B was introduced in the filtering plane, it passed all the frequencies of the object and hence the detector output showed maximum value. This can be verified from the Fig 4.10 (b). The image formed is very much

identical to the object light incident at the plane P_1.

When the filter 1 was introduced it blocked most of the higher spatial frequencies of the object and hence least light is transmitted. This can be seen in the Table 3. The consequent image formed is shown in Fig 4.10 (a).

When filters 2, 3 and 4 were introduced they transmitted all the lower and some of the higher spatial frequencies of the object and hence the detector output recorded was also close to maximum. The resultant image formed has lot of distortions due to absence of the higher spatial frequencies. This can be seen in Fig 4.10 (c), (d) and (e).

The same argument can be applied to all the other types of fingerprints too.

CHAPTER 5

CONCLUSIONS AND SUGGESTIONS

The experimental investigations described in the above chapters show that the Filtering and θ-Fourier methods have some advantages and disadvantages inherent to Coherent Optical system. They are discussed below.

5.1 FILTERING TECHNIQUE:

Fingerprints looking very similar but having little difference in the orientation of their ridge pattern can be best distinguished from their Fourier Spectra. Depending on the orientation of their ridge pattern the Fourier energy move around a circle with their central spot remaining the same in its position (see Fig 4.1 to Fig 4.5). For example, the fingerprints of the Right Hand and Left Hand thumb of a person looks very similar. The identification is very difficult in SEM and Microscopic study but it is best distinguished from their Fourier spectra in our method (See Fig 4.1 and Fig 4.4). The Fourier Spectra has the following unique characteristics.

The object can be moved laterally and vertically and can be translated axially in the light beam within the paraxial approximation without changing the position of its Fourier transform.

On the other hand, it is clear that this method has some weak points, too. They are

1. The light transmitted by the spatial filter introduced at P_2 during recognition process not only reconstructs the image of the fingerprints which are recognised, several other components are also present. These unwanted components produce ghost images which are

superimposed on the recognised image causing the desired image to become unintelligible by reducing the contrast of the image.

2. Moreover little difference in the magnitude of light transmitted by the filter contribute subtle changes in the image pattern. This cannot be observed by naked eye, causing recognition difficult.

3. Another problem faced by us is that when the Fourier transform of the object introduced at P_1 is a small arc with gaps on sides as shown in Fig 4.1 , it gets transmitted through all the filters introduced at the plane P_2 causing the recognition process extremely difficult.

5.2 θ-FOURIER METHOD:

The first two drawbacks mentioned above have been surmounted to some extent using θ-Fourier method.

This method is invariant to some pattern distortions and fairly good separability for a given set of patterns.

This method does not preserve any information about the position of the pattern in the input plane since only intensity variations are measured.

The advantages of this method, nevertheless may seem to outweigh its disadvantages mentioned above and hence fruitful results are obtained in this method.

5.3 SUGGESTION FOR FURTHER WORK

1. Recognition process can be made easier if a suitable filter

which can filter out the ghost images can be synthesized and introduced near the Fourier plane of the lens. So further work in the area of design of Optical Spatial filter will be of much use in the recognition process.

2. If a positive spatial filter transparent only in the portion where it was dark in the negative filter can be fabricated using contact print process then filtering process can be made very effective and better results can be obtained. This requires expertise and facilities which were not available to us.

CHAPTER 6

EXPERIMENTAL DETAILS AND PROCEDURE

To extract fingerprints from solid using laser light scattering method some vital things such as low power laser, beam expander, good quality large diameter lenses, neutral density filters and photodetector are required. The sample is mounted on a graduated rotating, translating table. Some of the salient features of the instrument are

1. One translational motion along the horizontal axis and rotational motion along the vertical axis are possible for the graduated table.

2. One translational motion along the horizontal axis for the whole system can be achieved by connecting the shaft of the assembly to a stepper-motor.

6.1 EXPERIMENTAL REQUIREMENTS

6.1.1 THE LASER

To keep the photodetector output in its linear range of operation a low power He-Ne coherent laser is used. The light falling on the surface of the specimen gets reflected in all directions since most of the surfaces available in nature are imperfect. Laser light are highly coherent and directional and hence is an ideal choice. A 0.95mW Spectra Physics laser is used in our experiment.

6.1.2 SELECTION OF DETECTING DEVICE

A P-I-N Phototransistor detector sensitive to 6328 Å is chosen

CHAPTER 6

EXPERIMENTAL DETAILS AND PROCEDURE

To extract fingerprints from solid using laser light scattering method some vital things such as low power laser, beam expander, good quality large diameter lenses, neutral density filters and photodetector are required. The sample is mounted on a graduated rotating, translating table. Some of the salient features of the instrument are

1. One translational motion along the horizontal axis and rotational motion along the vertical axis are possible for the graduated table.

2. One translational motion along the horizontal axis for the whole system can be achieved by connecting the shaft of the assembly to a stepper-motor.

6.1 EXPERIMENTAL REQUIREMENTS

6.1.1 THE LASER

To keep the photodetector output in its linear range of operation a low power He-Ne coherent laser is used. The light falling on the surface of the specimen gets reflected in all directions since most of the surfaces available in nature are imperfect. Laser light are highly coherent and directional and hence is an ideal choice. A 0.95mW Spectra Physics laser is used in our experiment.

6.1.2 SELECTION OF DETECTING DEVICE

A P-I-N Phototransistor detector sensitive to 6328 Å is chosen.

Responsivity of the detector is caliberated and due caution is exercised that the detector output never exceeds the saturation voltage of 200 mV. The angle subtended by the detector on the specimen surface needs to be small and hence the distance of the photodetector from the lens L_2 is adjusted such that the spotsize at the photodetector is less than the aperture area of the detector.

6.1.2 SELECTION OF BEAM EXPANDER

The laser beam coming out directly from the Spectr Physics laser is focussed using a biconvex lens L_1. The minimum diffraction limited spot-size that can be achieved is given by

$$d \cong f.\phi \qquad \ldots\ldots\ldots\ldots\ldots\ldots\ldots\ldots\ldots\ldots\ldots\ldots (22)$$

where

d = Diameter of the laser beam focussed by the lens

ϕ = beam divergence and is equal to 1.27 λ/D.

Here D refers to diameter of the laser beam waist

Equation (22) indicates that focussing laser light down to small spots can be accomplished with lenses of short focal length and laser with small beam divergence. The beam divergence of the laser, usually determined at the time the laser is designed, can still be reduced with the additional optics found in beam expanders.

A laser beam of width W_1 and beam divergence ϕ_1 is focussed by the first lens of the beam expander to a spot size of $d = f_1\phi_1$. The second lens, a distance f_2 from the focussed spot with $f_2 > f_1$ collects the light expanding from the focussed spot and essentially recollimates it. The beam divergence of the expanded, recollimated beam is equal to (see Fig 6.1)

$$\phi_2 = \left(\frac{W_1}{W_2}\right)\phi_1 = \left(\frac{f_1}{f_2}\right)\phi_1 \qquad \ldots\ldots\ldots\ldots\ldots\ldots (23)$$

where f_2/f_1 is the beam expansion ratio

By the principle of reversibility of light, if the expanded beam were to be redirected to the left and focussed by the second lens, it would form an identical spot at the same location so that $d_2 = f_2 \phi_2$ since $d_1 = d_2$ necessarily

$$f_1 \phi_1 = f_2 \phi_2$$

$$\phi_2 = \left[\frac{f_1}{f_2} \right] \phi_1 \qquad \text{.....(21)}$$

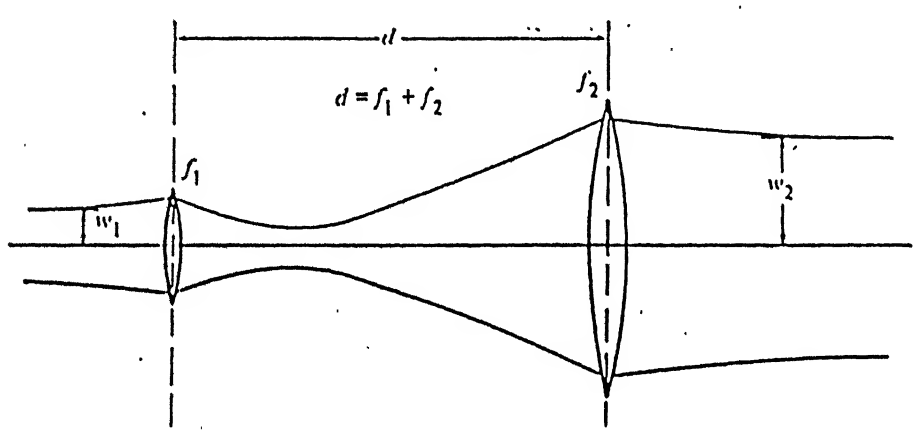

FIG 6.1 SCHEMATIC DIAGRAM OF A BEAM EXPANDER

If the beam expansion ratio is $f_2/f_1 = 10$ the beam divergence of the expanded laser beam is 1/10th that of the incident beam. Hence a beam expander of expansion ratio 10 is chosen.

6.1.4 SELECTION OF LENS L_1

To get scattering of light exclusively from the fingerprint, the spot size of the laser beam should be equal to or less than the thickness of the ridge pattrens. So different fingerprints have been observed through travelling microscope and the thickness of their ridges are measured. The table 4 shown below gives the minimum ridge thickness measured for various fingerprints. In addition the size of

the laser spot is measured at two different distances on its path of travel using knife edge experiment and the spotsize of the laser at any particular distance is calculated. Knowing the size of the spot at two

TABLE 4

SAMPLE	THICKNESS OF THE RIDGES (in cms)
A	0.007
B	0.010
C	0.012
D	0.008
E	0.019

different places, one before the focussing lens and another exactly at the front focal plane(Here the spot size is assumed to be equal to the difference between two ridges), the focal length of the lens L_1 is calculated using a simple Computer program shown in Appendix. The schematic diagram used for the focal length calculation is shown below in Fig 6.2.

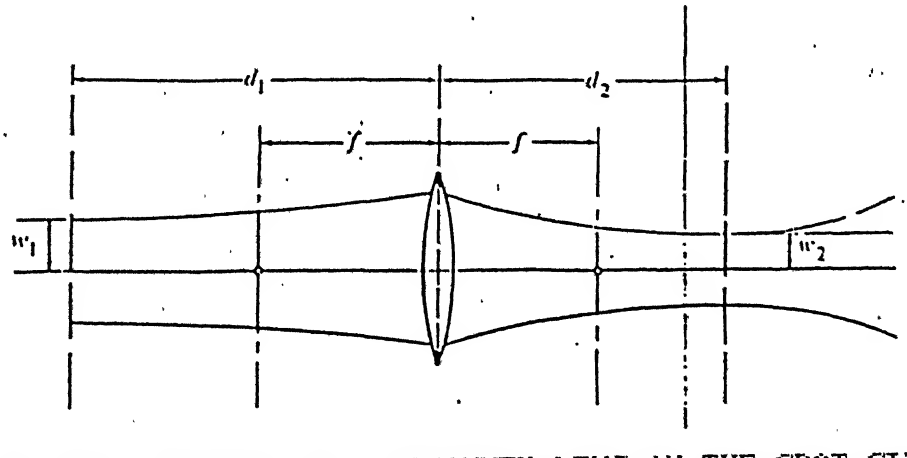

FIG 6.2 EFFECT OF A BICONVEX LENS ON THE SPOT SIZE

$$\left[\frac{1}{\omega_2^2}\right] = \frac{1}{\omega_1^2}\left[1 - \frac{d_1}{f}\right]^2 + \frac{1}{f^2}\left[\frac{\pi\,\omega_1}{\lambda}\right]^2 \quad \ldots\ldots\ldots(25)$$

where

$$\omega_1 = 0.125 \times 10^{-2}\ \text{m}$$
$$\omega_2 = 0.0035 \times 10^{-2}\ \text{m}$$
$$d_1 = 15 \times 10^{-2}\ \text{m}$$
$$\lambda = 6328 \times 10^{-10}\ \text{m}$$

From these values the focal length of the lens is calculated.

6.1.5 SELECTION OF LENS L_2

The laser light beam after falling on the specimen gets reflected specularly due to imperfection in the soild. So to collect maximum scattered light the diameter of the lens L_2 should be higher. The focal length of the lens should be such that at the focal plane of the lens the size of the spot should be smaller than the aperture area of the photodetector so that all the focussed light falls within the aperture area. Hence short focal length lens is chosen.

6.1.6 STEPPER-MOTOR AND DRIVING ASSEMBLY

The specimen mounted on the graduated rotating table is translated by connecting the shaft of the translational stage to a stepper motor. The specifications of the stepper motor is given below in Table 5. To avoid sideward motion of the motor during its operation, it is tightly fixed to the supporting table with magnetic mounts. The stepper motor is driven by a driver assembly. Signal to the driver assembly is given by a Personal Computer. The speed,duration and direction of the stepper motor can be varied by

TABLE 5

SPECIFICATIONS OF THE STEPPER MOTOR	
Type	STM 601
Input	12 V
Torque	2 Kg-Cm
V DC	0.5

6.1.7 PLOTTER AND SIGNAL PROCESSOR

Graphical form of the fingerprint pattern can be obtained from the HIOKI 8801 MEMORY HI CORDER . This is a flexible tool and so the photodetector output is connected to this plotter.

The output of the photodetector also goes to BOXCAR SIGNAL PROCESSOR. This samples the signal for a duration specified in it and stores it in a floppy. The input conditions selected for storing the signal is summarised below in Table 6.

Curve length	=	8192
Measurement	=	Static gate
Sample point	=	1 ms
Gate-width	=	755 ns
Input condition	=	DC, 1 M , 5V
Averaging	=	Live
Trigger mode	=	Free run
Preaveraging	=	Off
Sample rate	=	9.94 Hz
Run time	=	6 minutes
Time base	=	2 msec

The BOXCAR is a powerful device which can perform many

operations such as curve smoothening, subtraction and addition of data points etc.,

The following Fig 6.3 shows the Front view of the SINGAL PROCESSOR.

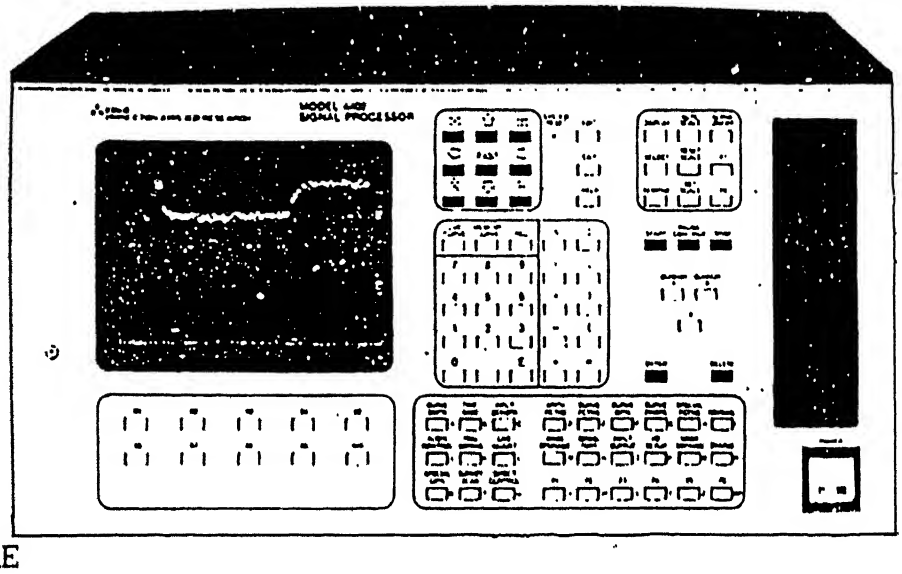

6.2 PROCEDURE

Fig 6.3 shows the schematic diagram of the experimental set-up. The sample (metal piece with fingerprint impression) is placed on a rotating graduated table. Laser beam after passing through the beam expander and biconvex lens L_1 of very short focal length gets focussed on to the fingerprint surface at an angle of 30° from the normal. The metal piece is kept at a distance of 24 cms from the laser. The spot size achieved on the specimen surface is about 1μm in diameter.

The light reflected from the metal surface therefore travels back along 30° on the opposite side of the normal if the surface is smooth enough. The scattered light is collected by lens L_2 kept at a distance of 12.5 cms from the metal piece and it is focussed on to the circular aperture of the photodetector opening.

The reflectivity of Brass and Aluminum surface are much higher than that of steel and hence appropriate neutral density filters have to be introduced between the lens L_2 and the photodetector to keep the operating voltage in the linear range of the detector. The detector is

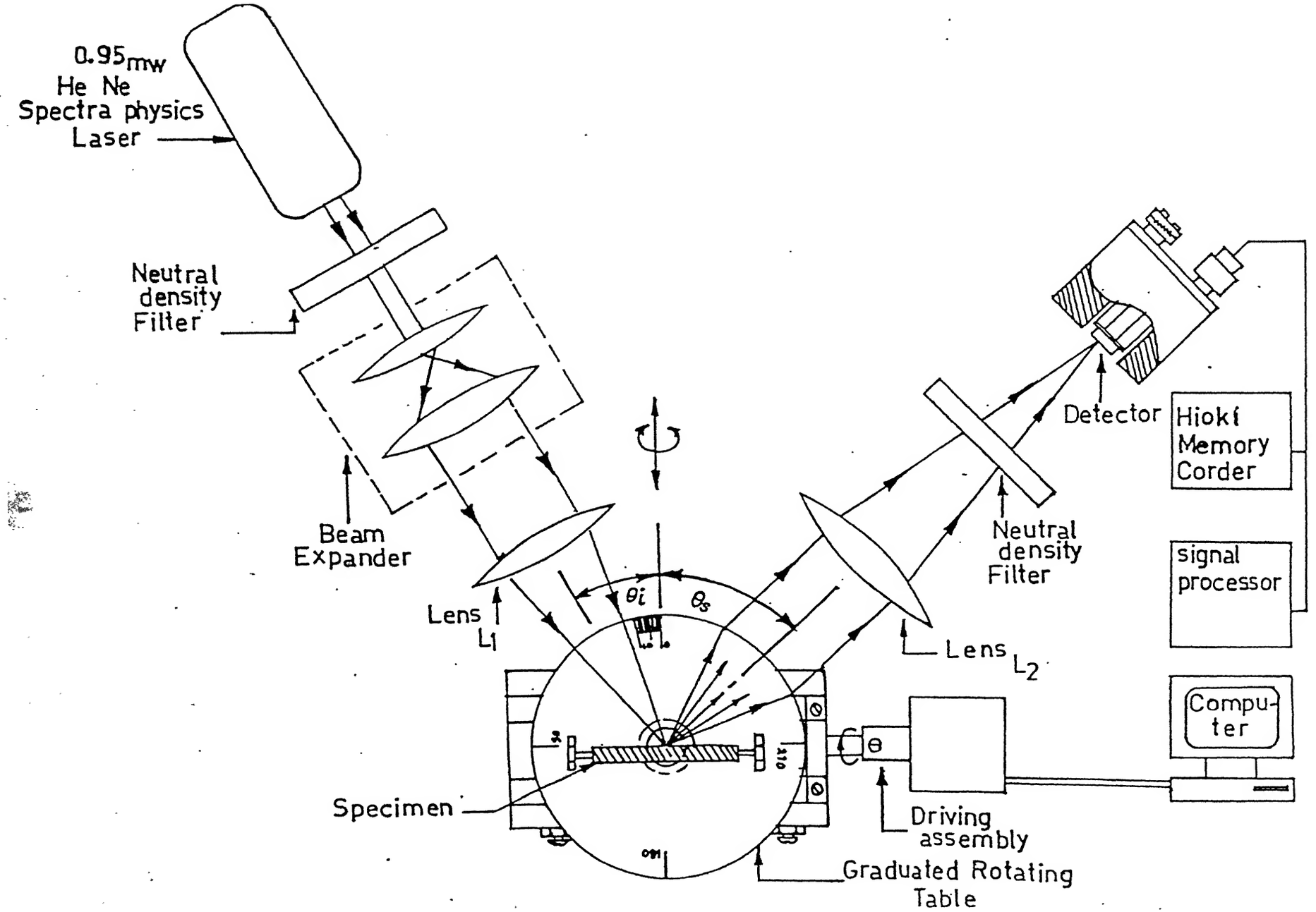

FIG 6.3 SCHEMATIC TOP VIEW OF THE EXPERIMENTAL SET-UP

very sensitive to stray light and hence the whole experiment is performed in dark.

6.3 MEASUREMENT OF THE SCATTERED INTENSITY

After aligning the whole experimental set-up, the mount on which the metal piece is kept is translated at an uniform rate of 5 rpm using the stepper motor. The laser light traverse from one end of the specimen where there is no fingerprint impression, then scans the whole portion of the fingerprint and reaches the other end of the specimen. The reflected light will be diffuse or specular depending on the nature of the surface. The incident laser light gets reflected from the surface of the metal piece due to fingerprint impression and surface irregularities, show marked variations in the photodetector output. The chart recorder driven at a speed of 5 secs /div. The photodetector output is simultaneously plotted using chart recorder as well as stored in the signal processor.

As soon as the laser light reaches one end of the specimen the stepper motor is stopped. The impression present on the metal surface is erased gently using non-reactive chemicals such as Acetone, Methanol etc., without disturbing the position of the metal piece. The laser light is then allowed to scan the same portion of the specimen surface in the same direction as before and the detector output is Plotted as well as stored. The same process is repeated for different metallic surfaces like Brass, Aluminum, Painted steel etc., with and without fingerprint.

CHAPTER 7

RESULTS AND DISCUSSIONS

Reflections of the incident laser beam from a metallic surface have been studied with and without fingerprints for one particular angle of incidence 30°. Different metallic surfaces such as Painted Steel, Aluminum, Brass and Polished aluminum are used as specimen and the results obtained from them for different fingerprints are shown in the following figures.

7.1 RETRIEVAL OF INTELLIGENCE FROM NOISE

The magnitude of scattering due to fingerprints is much smaller than that of the surface irregularities or imperfections. So one has to go for extraction of intelligence from noise using digital filtering techniques. To avoid complexi ty a simple way of extracting intelligence from noise was tried.

7.1.1 CASE I:

When the specimen with fingerprint impression on it is scanned with laser light the output of photodetector contains three contributions.

1. Variation due to fingerprint scattering which we call intelligence.
2. Variation due to surface irregularities. This is of no concern to us and hence it is named as noise(1).
3. Variation due to stray light, vibration of the specimen, laser noise etc., all put together called noise(2).

7.1.2 CASE II:

If the specimen is scanned again in the identical place as that of case I but without fingerprint impression, the detector output contain the following contributions

1. Variation due to surface irregularities

2. Variation due to straylight, vibration of the specimen, laser noise etc.,

Subtraction of the detector output obtained in the second case from that of the first case gives us intelligence

[INTELLIGENCE + NOISE (1) + NOISE (2)] - [NOISE(1) + NOISE(2)] =

INTELLIGENCE

Before doing subtraction one has to match starting and end points of both the signals so that one-to-one correspondence is established. The value of intelligence after subtraction shows almost zero amplitude in the beginning as well as in end of the signal.This due to fact that the laser beam scanned only empty surface in both the cases Since the impression of the fingerprint is very weak in the metallic surface the signal amplitude is correspondingly less. The above said technique is applied to various fingerprints and the results obtained are shown below.

CHAPTER 8

CONCLUSIONS AND SUGGESTIONS

8.1 CONCLUSIONS

The magnitude of scattering of laser light is much higher in the case of Aluminum and Brass compared to scattering due to fingerprint impression and hence subtraction operation becomes crucial. Any mismatch in the starting point of both the signals of Case I and case II will lead to misleading result. To check the veracity of the result the experiment is repeated many times.

Scattering of light from solid takes place at the microscopic level.So any change in the position of the specimen will give an entirely different result.Moreover the magnitude of scattering due to fingerprints depend on its contrast and hence degraded latent prints give signal whose magnitude is much smaller than noise, making signal extraction process rather tedious.

Despite all the aforesaid drawbacks we could get some results in our method. In the subtraction operation all the common noise present in both the signals of Case I and Case II gets eliminated. Transfer of data from signal processor to personal computer could not be carried out due to non-availability of proper interface card and program and so noise elimination process got impeded.

Matching two similar fingerprints using Microscopic and SEM methods is very laborious. Instead comparison can be done within no time in our graphical method. The ridge spacing doesn t vary much even when the fingerprints are scanned at slightly different direction,making the comparison process easy. Matching can also be

established even for imcomplete fingerprints. If the detector output of the fingerprints can be stored and comparisons can be performed in a Personal Computer results can be obtained at faster rate.

8.2 SUGGESTIONS FOR FURTHER WORK

The vibrations of the Stepper motor gets transmitted to the sample through the shaft of the translational stage and this causes variation in the detector output. This vibration contributes higher frequency noise to the signal which may be eliminated using a digital filter.

Much work can be done on the signal extraction part to improve the signal using filtering techniques.

REFERENCES

1. J. Godsell, Fingerprint Techniques. *Journal Of Forensic Science Science Society* (1961),79

2. J.L. Peterson, Utilising the Laser for Comparing Tool Striations. *Journal of Forensic Science Society* (1974),57

3. G. E. Garner, C. R. Fontan and D. W. Hobson, Visualisation of Fingerprints in the Scanning Electron Microscope, *Journal Of Forensic Science Society* (1975),281

4. Neil Collings (1985), *Optical Pattern Recognition using Holographic Techniques*, Addison-Wesley Publishing Company

5. P. Hariharan (1986), *Optical Holography Principles, Techniques and Applications*, Cambridge University Press

6. E.G. Steward (1983), *Fourier Optics an Introduction*, John Wiley & Sons

7. K. Lizuka (1985), *Engineering Optics*, Springer-Verlag.

8. Neil Collings, *Optical Pattern Recognition using Holographic Techniques*, Addison-Wesley Publications

General Reference

1. Fred Unterseher, Jeannene Hansen, Bob Schlesinger (1982), *Holography Handbook*, Ross Books

2. K.D. Moller (1988), *Optics*,

3. H. Lipson (1972), *Optical transforms*, Academic Press

4. Eugene Hecht (1987), *Optics*, Addison-Wesley Pulications

5. S.H. Lee (1981), *Optical Information Processing Fundamentals*, Springer-verlag

6. J.D. Armitage and A. W. Lohmann, Character Recognition by Incoherent Spatial Filtering, *Applied Optics* (1965), 461

7. R. A. Binns, A. Dickinson and B. M. Watrasiewicz, Methods Of

Increasing Discrimination in Optical Filtering, *Applied Optics* (1968),1047

8. Sing H. Lee, The Synthesis Of Complex Spatial Filters for Coherent Optical Data Processing, *Pattern Recognition* (1972),21

9. A. Vander Lugt, The Effect of Small Displacements of Spatial Filters, *Applied Optics* (1967),1221

10. George G. Lendaris and Gordon L. Stanley, Diffraction Pattern Sampling for Automatic Pattern Recognition, *Proceedings of the IEEE* (1970),198

11. J. W. Goodman , *Introduction to Fourier Optics*

12. M. Francon (1979), *Optical Image Formation and Processing*, Academic Press

13. M. Young (1977), *Optics and Lasers*, Springer-Verlag

APPENDIX

Program 1:

```
c       ** PROGRAM TO FIND FOCAL LENGTH OF A LENS **
        Real d1,w1,w2,l,pnu,pdi,ptot1,ptot2,pint
        Open (unit=44,file='lens.out')
        Read (*,*) w1,w2,l
        d1 = sqrt((d1**2+(1000*3.14**2
     1  *l**4)/l**2))
        pdi = 2*(10*(w1**2/w2**2)-1)
        ptot1 = (d1**2 + pnu)/pdi
        ptot2 = (d1**2 - pnu)/pdi
        write (22,2)ptot1,ptot2
        print*,ptot1 ptot2
 2      format(1x,'The two focal length are',2e13.4,2x,'meters')
        stop
        end
```

INPUT VALUES

d1= 3 w1= 0.000600 , w2= 0.0000035 , l= 0.0000006328

(ALL IN METRES)

OUTPUT VALUES:

THE FOCAL LENGTH OF THE LENS :0.1042 metres

Program 2:

```
c       ** PROGRAM TO FIND THE DISTANCE OF THE SECOND WAIST **

        Real w1,w2,l,pnum,pdinum,pres,d2
        open (unit=22,file='lens2.out')
        Read (*,*)d1,w1,l,f
        pnum = (d1**2-f1*f**2
        pdinum = ((d1**2-f1**2 + ((3.14 * w1 **2)/l)**2)
        pres = pnum/pdinum
        d2 = f + pres
        write (22,2)d2
        print *,d2
 2      format (1x,'The distance from lens to w2',f9.4,2x,'metres')
        stop
        end
```

INPUT VALUES:

d1= 0.3 , w1= 0.000600 , w2= 0.0000035 , l= 0.0000006328

(ALL IN METRES)

OUTPUT VALUES:

THE FOCAL LENGTH OF THE LENS :0.1042 metres

LTP-1992-M-MUT-OPT